# Biomedisinsk instrumentering – faselåseforsterker, elektroder og endogene biopotensialer

**Apparatur:** Multimeter, faselåseforsterker, EKG-monitor, elektroder, lagrings-oscilloskop.

---

Endogene biopotensialer er de potensialer som kroppen selv genererer. I denne oppgaven skal vi se litt på slike potensialer og hvordan de kan plukkes opp med elektroder på hudoverflaten. Ved hjelp av en faselåseforsterker (FLF) (lock-in amplifier) skal vi måle hudens admittans. Vi skal dessuten se på EDR (ElektroDermal Respons) -aktivitet, som bl.a. måles ved diagnostisering av psykiske og nevrofysiologiske lidelser, og ved løgn-deteksjon. Først må vi se på FLF og måleteknikken som ligger til grunn.

## 1. Måleoppstilling med faselåseforsterker (FLF)

**Måleprinsipp**
Vi skal finne en ukjent admittans $Y$. $Y$ er en kompleks størrelse som kan karakteriseres ved sin modul $|Y|$ (siemens) og fasevinkel $\Theta$. Admittansen $Y$ er den inverse av impedansen $Z$:

$$Y = \frac{1}{Z} \qquad (Y \text{ i siemens}, Z \text{ i ohm})$$

Vi bruker en målekrets med en konstant spenningskilde med amplitude $v$ og frekvens $f$, og måler resulterende strøm $i$ (fig.1).

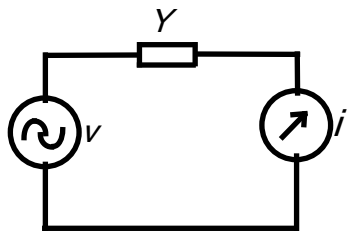


**Fig.1: Målekrets, prinsippskjema.**

Vi vil finne den ukjent admittansen $Y$. Den blir etter Ohms lov:

$$Z = \frac{v}{i} \qquad\qquad Y = \frac{i}{v}$$

Med den måleoppstilling vi bruker, måles *i* med FLF, og vi ser at det er proporsjonalitet mellom *Y* og *i* (ikke mellom *Z* og *i* !). Vi avleser |*i*| og fasevinkelen Θ, og beregner deretter |*Y*| [S].

**Faselåseforsterkeren (FLF), Stanford Research 830**

Stanford Research 830 er en digital FLF som inneholder både oscillatoren og strømforsterkeren i fig.1. Strømforsterkeren etterfølges av forskjellige filtre og deretter en 18 bits A/D-omformer. Verdiene fra A/D-omformeren blir multiplisert med henholdsvis oscillatorspenningen (sinus) og en spenning som er dreid 90° i forhold til denne (cosinus) for å få separert ut realdel (i fase) og imaginærdel (90° ut av fase) av den målte strømmen. Realdelen (Re *i*) vil nå være proporsjonal med den målte konduktansen, og imaginærdelen (Im *i*) vil være proporsjonal med den målte suseptansen (denne vil for biologisk vev alltid være kapasitiv).

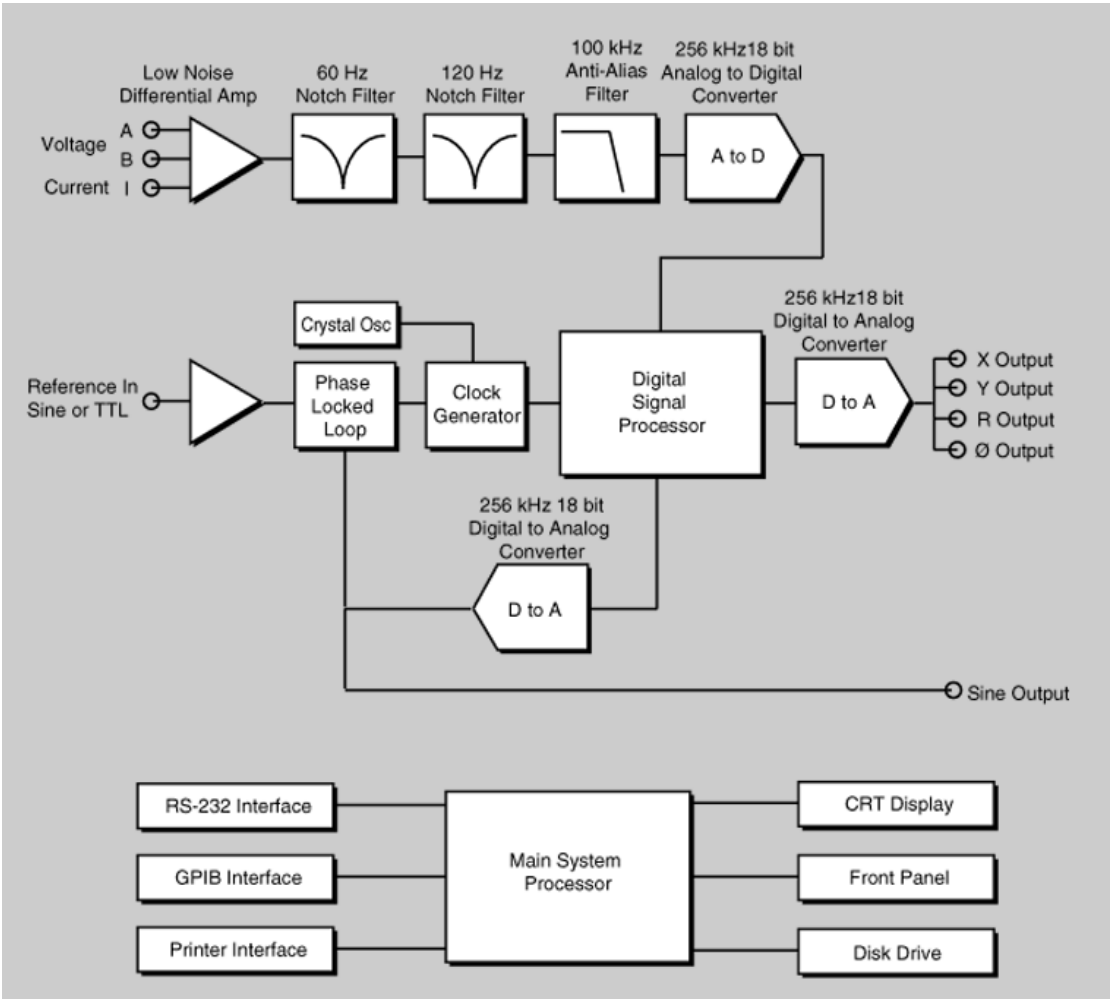


**Fig.2: Digital faselåseforsterker, blokkskjema.**

Oscillatorutgangen er til høyre på frontpanelet (se siste side). Oscillatorens frekvens, amplitude og fase kan stilles ved først å trykke på den aktuelle tasten, og så stille inn ønsket verdi med hjulet. Det er også mulig å velge hvilken av de harmoniske komponentene man vil måle, og denne må stå innstilt på 1. harmoniske. Det å velge en fase for oscillatoren som er forskjellig fra null, betyr at den spenningen som multipliseres med målesignalet blir fasedreid i forhold til oscillatoren. Dette kan brukes hvis man har en kjent fasedreining i målesystemet som man ønsker å kompensere for.

Strømforsterker-inngangen er til venstre på frontpanelet. Man benytter BNC-kontakten merket A/I, og velger med Input-knappen I($10^6$). Følsomheten (sensitivity) settes til en høy verdi i utgangspunktet (lav følsomhet), og justeres etter at målingen har begynt til en verdi hvor skalaen utnyttes mest mulig uten at man får "overload". Hvis man f.eks. måler 167 nA, vil det være riktig å sette "sensitivity" til 200 nA.

Etter strømforsterkeren er det bl.a. filtre som fjerner nettfrekvensen (50 og 100 Hz). Disse skal ikke være innkoblet i denne oppgaven.

Vi kan velge om FLF skal vise resultatet som realdel og imaginærdel, eller som modul og fasevinkel. Mellom multiplikatorkretsene og utgangene er det koblet inn et lavpassfilter slik at vi får et pent DC-signal ut. Filterets tidskonstant kan velges øverst til venstre på SR830. Velg f.eks. 1 sek. på de høyere målefrekvensene og 3 eller 10 sek. på de lavere.

## 2. Elektrodene

Selve elektrodene er overgangen mellom elektronisk og ionisk ledning. Les mer om dette i det vedlagte utdraget om elektroder. I de elektrodene vi skal bruke, er overgangen møtet mellom en sølv/sølvklorid overflate (fiolett farge) og en elektrolyttgelé med klor-ioner. Det er også en limflate som fester elektrodene til huden.

Et elektrodepar kan elektrisk karakteriseres ved generert DC-spenning V og en kompleks admittans Y. Den siste er en funksjon av frekvensen.

**Målinger.**
Fest to elektroder rett mot hverandre. Vi får da bidraget fra to elektroder i serie.

- Mål DC-potensial med multimeteret. Virker potensialet stabilt? Er det temperatur- eller trykk-avhengig?

- Vi skal ikke måle admittansen for elektrodenen i denne oppgaven, og forutsetter at den er mye høyere enn admittansen i huden.

## 3. Endogene DC-potensialer

Fest to elektroder til samme arm. En elektrode på innsiden av underarmen og en på indre håndflate på tommelfingermuskelen. Mål med multimeteret DC-spenningen mellom elektrodene. Hvilken polaritet har håndflaten i forhold til underarmen? Hvor stort er elektrodenes eget potensial (som målt under pkt.2), som feilkilde?
Prøv så å framkalle endringer i DC-spenningen ved først å sitte helt rolig og avslappet i ca. 30 sek., og så skvette til i stolen mens du trekker pusten fort og dypt. Prøv imidlertid å ikke bevege for mye på armen hvor elektrodene er tilkoblet. Beskriv hva som skjer med DC-spenningen.

## 4. Hudadmittans

Det øverste døde hudlaget (hornhuden), som er 10-100μm tykt, har svært lav admittans i forhold til resten av huden. Den admittansen vi måler med en overflateelektrode kan derfor tilnærmet sies utelukkende å gjenspeile hornhudens tilstand. Dersom du måler admittansen mellom elektrodene du har festet på armen, måler du altså ledningsevnen til hornhuden under de to elektrodene i serie, som i fig.3 (i tillegg til admittansen i elektrodene).

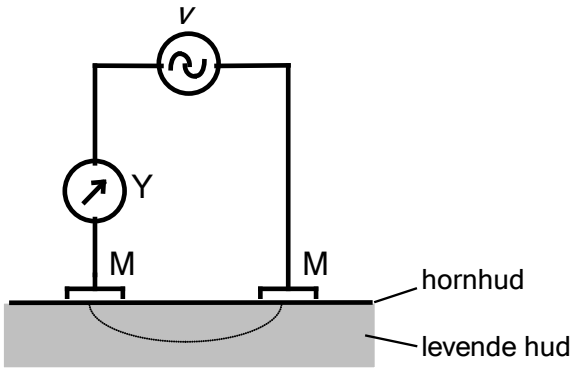


**Fig.3: To-elektrodesystem på hud.**

Dette blir altså en bipolar måling, fordi vi måler på to hudområder i serie. Hvordan tror du vi kunne oppnå en unipolar måling (ett hudområde) ved å endre på størrelsen på en av elektrodene?

En bedre måte å oppnå en unipolar måling på, er å innføre en operasjonsforsterker og en tredje elektrode, som i fig.4, hvor elektrodene er kalt M for "measuring electrode", C for "current carrying electrode" of R for "reference electrode".

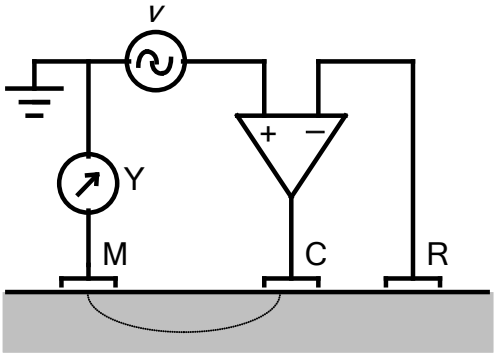


**Fig.4: Tre-elektrodesystem på hud.**

Vi får nå hele målespenningen *v* over hornhuden som er under elektrode M, og strømmen *i* vil altså være proporsjonal med admittansen under denne elektroden. **Prøv å forklare hvorfor.**

Fest en elektrode til inne i håndflaten, og koble de to elektrodene i håndflaten til henholdsvis oscillatorutgangen og strøminngangen på FLF.

Koble utgangene fra FLF (CH1 OUTPUT og CH2 OUTPUT) til inngangene på et lagrings-oscilloskop. De to display'ene på FLF skal nå settes opp til å vise real- og imaginærdel (h.h.v. X og Y). Mål nå admittansen ved 20Hz, 10mV. Still inn oscilloskopet slik at du kan følge forløpene til konduktansen (G) og suseptansen (ωC ) i sanntid (langsomt sweep). Bruk

framgangsmåten under pkt.4 til å framkalle GSR-bølger. Er bølgene like store i G- og ωC -kanalen? Prøv å gi en kort beskrivelse av fenomenet.

Mål nå admittansen mellom en elektrode på høyre underarm og en elektrode på venstre underarm ved 1, 10, 100 og 1000 Hz. Presenter resultatene i en tabell slik:

| Frekvens: | Admittans: | Fasevinkel: | Konduktans: | Suseptans: |
|---|---|---|---|---|
| | | | | |
| | | | | |

Plott deretter konduktans og suseptans som funksjon av frekvens i et diagram med logaritmiske akser (Bode-diagram). Prøv å gi kommentarer til de forløpene du finner.

## 5. Hjerterytme - EKG

Bruk nå en elektrode på den ene underarmen og to elektroder på den andre underarmen. Koble til EKG-monitoren. Avgjør hvilken elektrode-ledning som er referanse og hvilke to som plukker opp biopotensialforskjellen. Finn EKG-signalet, avles amplituden og hjertefrekvens. Prøv å oppnå stabil hjertefrekvens. Noter hjertefrekvensen f.eks. hver 10. sek. Gjør så noen knebøyninger og tegn et diagram over hjertefrekvens som funksjon av tid. Merk av med pil når knebøyningene starter og slutter. Gi en kort beskrivelse av kurven du finner.

## 6. Elektromyografi (EMG)

Velg en avledning slik at det ikke er EKG-signal på skjermen. Stram musklene i armen og finn de elektriske muskelpotensialene (EMG). Hva er amplitude og frekvensinnholdet grovt anslått ut fra skjermbildet? Hvordan stemmer frekvensinnholdet med det som er oppgitt i diagrammet bakerst i denne oppgaven? Hvis det ikke stemmer – hva tror du årsaken til dette kan være?

# FRONT PANEL

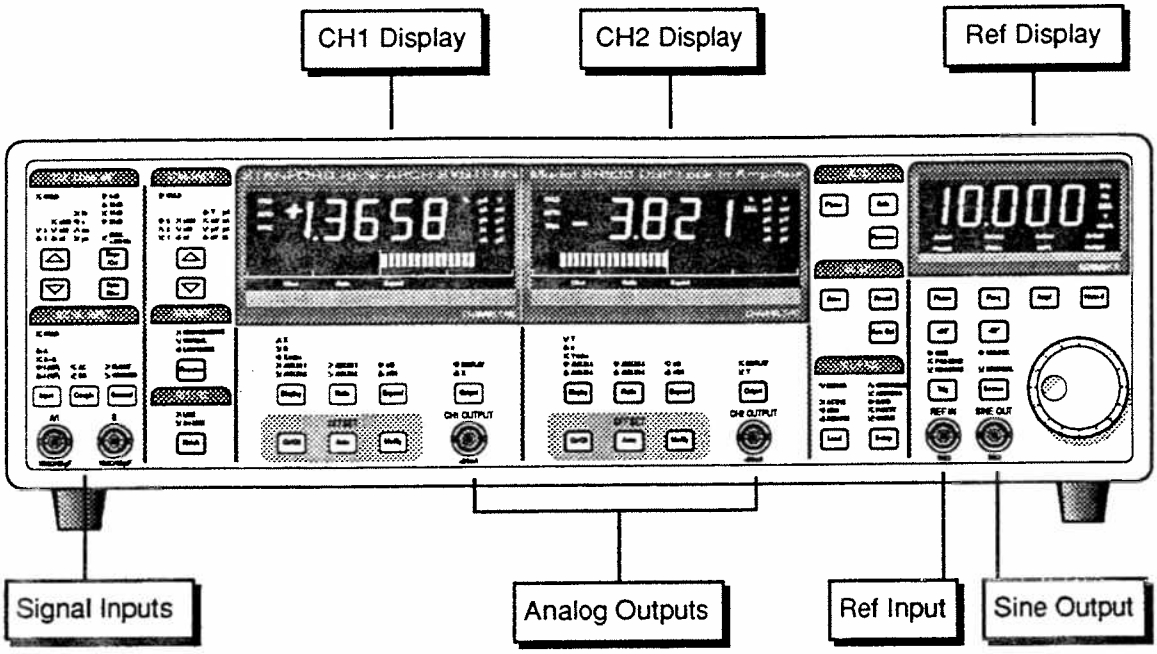
CH1 Display
CH2 Display
Ref Display
Signal Inputs
Analog Outputs
Ref Input
Sine Output

# WHAT IS A LOCK-IN AMPLIFIER?

Lock-in amplifiers are used to detect and measure very small AC signals - all the way down to a few nanovolts! Accurate measurements may be made even when the small signal is obscured by noise sources many thousands of times larger.

Lock-in amplifiers use a technique known as phase-sensitive detection to single out the component of the signal at a specific reference frequency AND phase. Noise signals at frequencies other than the reference frequency are rejected and do not affect the measurement.

## Why use a lock-in?

Let's consider an example. Suppose the signal is a 10 nV sine wave at 10 kHz. Clearly some amplification is required. A good low noise amplifier will have about 5 nV/√Hz of input noise. If the amplifier bandwidth is 100 kHz and the gain is 1000, then we can expect our output to be 10 μV of signal (10 nV x 1000) and 1.6 mV of broadband noise (5 nV/√Hz x √100 kHz x 1000). We won't have much luck measuring the output signal unless we single out the frequency of interest.

If we follow the amplifier with a band pass filter with a Q=100 (a VERY good filter) centered at 10 kHz, any signal in a 100 Hz bandwidth will be detected (10 kHz/Q). The noise in the filter pass band will be 50 μV (5 nV/√Hz x √100 Hz x 1000) and the signal will still be 10 μV. The output noise is much greater than the signal and an accurate measurement can not be made. Further gain will not help the signal to noise problem.

Now try following the amplifier with a phase-sensitive detector (PSD). The PSD can detect the signal at 10 kHz with a bandwidth as narrow as 0.01 Hz! In this case, the noise in the detection bandwidth will be only 0.5 μV (5 nV/√Hz x √.01 Hz x 1000) while the signal is still 10 μV. The signal to noise ratio is now 20 and an accurate measurement of the signal is possible.

## What is phase-sensitive detection?

Lock-in measurements require a frequency reference. Typically an experiment is excited at a fixed frequency (from an oscillator or function generator) and the lock-in detects the response from the experiment at the reference frequency. In the diagram below, the reference signal is a square wave at frequency $\omega_r$. This might be the sync output from a function generator. If the sine output from the function generator is used to excite the experiment, the response might be the signal waveform shown below. The signal is $V_{sig}\sin(\omega_r t + \theta_{sig})$ where $V_{sig}$ is the signal amplitude.

The SR830 generates its own sine wave, shown as the lock-in reference below. The lock-in reference is $V_L\sin(\omega_L t + \theta_{ref})$.

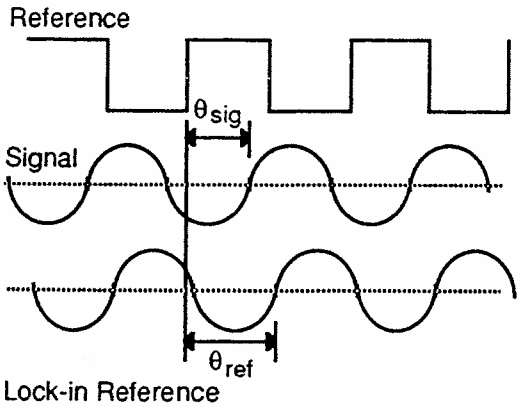

Lock-in Reference

The SR830 amplifies the signal and then multiplies it by the lock-in reference using a phase-sensitive detector or multiplier. The output of the PSD is simply the product of two sine waves.

$$V_{psd} = V_{sig}V_L\sin(\omega_r t + \theta_{sig})\sin(\omega_L t + \theta_{ref})$$

$$= 1/2\, V_{sig}V_L\cos([\omega_r - \omega_L]t + \theta_{sig} - \theta_{ref}) - 1/2\, V_{sig}V_L\cos([\omega_r + \omega_L]t + \theta_{sig} + \theta_{ref})$$

The PSD output is two AC signals, one at the difference frequency ($\omega_r - \omega_L$) and the other at the sum frequency ($\omega_r + \omega_L$).

If the PSD output is passed through a low pass filter, the AC signals are removed. What will be left? In the general case, nothing. However, if $\omega_r$ equals $\omega_L$, the difference frequency component will be a DC signal. In this case, the filtered PSD output will be

$$V_{psd} = 1/2\, V_{sig}V_L\cos(\theta_{sig} - \theta_{ref})$$

This is a very nice signal - it is a DC signal proportional to the signal amplitude.

## Narrow band detection

Now suppose the input is made up of signal plus noise. The PSD and low pass filter only detect signals whose frequencies are very close to the lock-in reference frequency. Noise signals at frequencies far from the reference are attenuated at the PSD output by the low pass filter (neither $\omega_{noise}$-$\omega_{ref}$ nor $\omega_{noise}$+$\omega_{ref}$ are close to DC). Noise at frequencies very close to the reference frequency will result in very low frequency AC outputs from the PSD ($|\omega_{noise}-\omega_{ref}|$ is small). Their attenuation depends upon the low pass filter bandwidth and roll-off. A narrower bandwidth will remove noise sources very close to the reference frequency, a wider bandwidth allows these signals to pass. The low pass filter bandwidth determines the bandwidth of detection. Only the signal at the reference frequency will result in a true DC output and be unaffected by the low pass filter. This is the signal we want to measure.

## Where does the lock-in reference come from?

We need to make the lock-in reference the same as the signal frequency, i.e. $\omega_r = \omega_L$. Not only do the frequencies have to be the same, the phase between the signals can not change with time, otherwise $\cos(\theta_{sig} - \theta_{ref})$ will change and $V_{psd}$ will not be a DC signal. In other words, the lock-in reference needs to be phase-locked to the signal reference.

Lock-in amplifiers use a phase-locked-loop (PLL) to generate the reference signal. An external reference signal (in this case, the reference square wave) is provided to the lock-in. The PLL in the lock-in locks the internal reference oscillator to this external reference, resulting in a reference sine wave at $\omega_r$ with a fixed phase shift of $\theta_{ref}$. Since the PLL actively tracks the external reference, changes in the external reference frequency do not affect the measurement.

## All lock-in measurements require a reference signal.

In this case, the reference is provided by the excitation source (the function generator). This is called an external reference source. In many situations, the SR830's internal oscillator may be used instead. The internal oscillator is just like a function generator (with variable sine output and a TTL sync) which is always phase-locked to the reference oscillator.

## Magnitude and phase

Remember that the PSD output is proportional to $V_{sig}\cos\theta$ where $\theta = (\theta_{sig} - \theta_{ref})$. $\theta$ is the phase difference between the signal and the lock-in reference oscillator. By adjusting $\theta_{ref}$ we can make $\theta$ equal to zero, in which case we can measure $V_{sig}$ ($\cos\theta$=1). Conversely, if $\theta$ is 90°, there will be no output at all. A lock-in with a single PSD is called a single-phase lock-in and its output is $V_{sig}\cos\theta$.

This phase dependency can be eliminated by adding a second PSD. If the second PSD multiplies the signal with the reference oscillator shifted by 90°, i.e. $V_L\sin(\omega_L t + \theta_{ref} + 90°)$, its low pass filtered output will be

$$V_{psd2} = 1/2\, V_{sig}V_L\sin(\theta_{sig} - \theta_{ref})$$

$$V_{psd2} \sim V_{sig}\sin\theta$$

Now we have two outputs, one proportional to $\cos\theta$ and the other proportional to $\sin\theta$. If we call the first output X and the second Y,

$$X = V_{sig}\cos\theta \qquad Y = V_{sig}\sin\theta$$

these two quantities represent the signal as a vector relative to the lock-in reference oscillator. X is called the 'in-phase' component and Y the 'quadrature' component. This is because when $\theta$=0, X measures the signal while Y is zero.

By computing the magnitude (R) of the signal vector, the phase dependency is removed.

$$R = (X^2 + Y^2)^{1/2} = V_{sig}$$

R measures the signal amplitude and does not depend upon the phase between the signal and lock-in reference.

A dual-phase lock-in, such as the SR830, has two PSD's, with reference oscillators 90° apart, and can measure X, Y and R directly. In addition, the phase $\theta$ between the signal and lock-in reference, can be measured according to

$$\theta = \tan^{-1}(Y/X)$$

# WHAT DOES A LOCK-IN MEASURE?

So what exactly does the SR830 measure? Fourier's theorem basically states that any input signal can be represented as the sum of many, many sine waves of differing amplitudes, frequencies and phases. This is generally considered as representing the signal in the "frequency domain". Normal oscilloscopes display the signal in the "time domain". Except in the case of clean sine waves, the time domain representation does not convey very much information about the various frequencies which make up the signal.

## What does the SR830 measure?

The SR830 multiplies the signal by a pure sine wave at the reference frequency. All components of the input signal are multiplied by the reference simultaneously. Mathematically speaking, sine waves of differing frequencies are orthogonal, i.e. the average of the product of two sine waves is zero unless the frequencies are EXACTLY the same. In the SR830, the product of this multiplication yields a DC output signal proportional to the component of the signal whose frequency is exactly locked to the reference frequency. The low pass filter which follows the multiplier provides the averaging which removes the products of the reference with components at all other frequencies.

The SR830, because it multiplies the signal with a pure sine wave, measures the single Fourier (sine) component of the signal at the reference frequency. Let's take a look at an example. Suppose the input signal is a simple square wave at frequency f. The square wave is actually composed of many sine waves at multiples of f with carefully related amplitudes and phases. A 2V pk-pk square wave can be expressed as

$$S(t) = 1.273\sin(\omega t) + 0.4244\sin(3\omega t) + 0.2546\sin(5\omega t) + \ldots$$

where $\omega = 2\pi f$. The SR830, locked to f will single out the first component. The measured signal will be $1.273\sin(\omega t)$, not the 2V pk-pk that you'd measure on a scope.

In the general case, the input consists of signal plus noise. Noise is represented as varying signals at all frequencies. The ideal lock-in only responds to noise at the reference frequency. Noise at other frequencies is removed by the low pass filter following the multiplier. This "bandwidth narrowing" is the primary advantage that a lock-in amplifier provides. Only inputs at frequencies at the reference frequency result in an output.

## RMS or Peak?

Lock-in amplifiers as a general rule display the input signal in Volts RMS. When the SR830 displays a magnitude of 1V (rms), the component of the input signal at the reference frequency is a sine wave with an amplitude of 1 Vrms or 2.8 V pk-pk.

Thus, in the previous example with a 2 V pk-pk square wave input, the SR830 would detect the first sine component, $1.273\sin(\omega t)$. The measured and displayed magnitude would be 0.90 V (rms) ($1/\sqrt{2} \times 1.273$).

## Degrees or Radians?

In this discussion, frequencies have been referred to as f (Hz) and $\omega$ ($2\pi f$ radians/sec). This is because people measure frequencies in cycles per second and math works best in radians. For purposes of measurement, frequencies as measured in a lock-in amplifier are in Hz. The equations used to explain the actual calculations are sometimes written using $\omega$ to simplify the expressions.

Phase is always reported in degrees. Once again, this is more by custom than by choice. Equations written as $\sin(\omega t + \theta)$ are written as if $\theta$ is in radians mostly for simplicity. Lock-in amplifiers always manipulate and measure phase in degrees.

# BIOIMPEDANCE AND BIOELECTRICITY BASICS

Sverre Grimnes, MSc PhD
*Department of Physics, University of Oslo and*
*Department of Biomedical and Clinical Engineering, Rikshospitalet, Oslo*

and

Ørjan Grøttem Martinsen, MSc PhD
*Department of Physics, University of Oslo*

ACADEMIC PRESS

A Harcourt Science and Technology Company

San Diego San Francisco New York
Boston London Sydney Tokyo

## 2.5. Electrodics and ac Phenomena

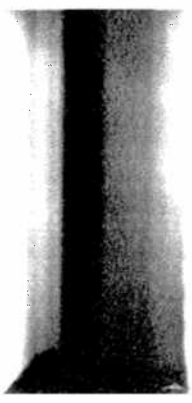

The *half-cell* concept is often used for analysing an electrode with its surrounding solution. However, we do not have access to an isolated half-cell, so a real

electrolytic cell consists of two half-cells. Often the second electrode is considered to be a reference electrode.

### 2.5.1. Electrode equilibrium dc potential, zero external current

**Metal/ion and redox systems**

According to Nernst, metals have a tendency to release their ions into a solution as solvated particles. The potential difference arises from this transfer of positive metal ions across the double layer, with a resulting negative potential on the metal electrode. The standard potentials of such *metal/ion* half-cells are shown in Table 2.9, where the reference electrode is the hydrogen electrode. Volta's original findings were in rough accordance with this table. The least noble metals have the most negative values. For the noble metals, the number of metal ions released into the solution may be small, and the potential must then be measured under strict zero-current conditions.

With an external dc power supply connected to the electrolytic cell, the applied voltage that gives *no dc current flow* in the external circuit corresponds to the *equilibrium potential* of the half-cell (or actually the cell). It is the same voltage as read by a voltmeter with very high input resistance and virtually no current flow (pH meter). In electrochemistry, *potentiometry* is the measurement of the potential of an electrode at zero current flow, that is when the cell is not externally polarised. In order to understand the equilibrium potential with zero external current, we must introduce the concept of electrode reaction, and link it with an electric current in the external circuit. An electrode reaction going rapidly both ways (ionisation/de-ionisation, reduction–oxidation) is called *reversible*. A pure redox system presup-

**Table 2.9.** Metal/ion equilibrium potentials

| Metal/metal ion | $V_0$ (volt) |
|---|---|
| $Li/Li^+$ | −3.05 |
| $K/K^+$ | −2.93 |
| $Na/Na^+$ | −2.71 |
| $Al/Al^{3+}$ | −1.66 |
| $Zn/Zn^{2+}$ | −0.76 |
| $Fe/Fe^{2+}$ | −0.44 |
| $Ni/Ni^{2+}$ | −0.25 |
| $Sn/Sn^{2+}$ | −0.14 |
| $Pb/Pb^{2+}$ | −0.13 |
| $H_2/H^+$ | **0** |
| Carbon | dependent on structure |
| $Cu/Cu^{2+}$ | +0.34 |
| $Ag/Ag^+$ | +0.80 |
| $Pt/Pt^{2+}$ | + ~1.2 |
| $Au/Au^{3+}$ | +1.50 |

poses an inert electrode metal, e.g. platinum, with no electrode metal ion transfer. At the electrodes the redox system is:

The *anode* is the *electron* sink, where ions or neutral substances lose electrons and are oxidised: red → ox + *ne*.

The *cathode* is the *electron* source where ions or neutral substances gain electrons and are reduced: ox + *ne* → red.

The metal/ion half-cell generates a potential by the exchange of *metal ions* between the metal and the electrolyte solution. In contrast, a *redox* half-cell is based upon an exchange of *electrons* between the metal and the electrolyte solution. So actually there are two sets of standard potential tables, one for metal/ion half-cells (Table 2.9), and one for redox half-cells (Table 2.10). The half-cell potential is of course *independent* of the interphase area, because equilibrium potential is without current flow. As soon as the cell is externally polarised and a current is flowing, electrode area is of interest (current density).

Table 2.10 shows some typical half-cell standard potentials for redox systems.

**The Nernst equation**

The Nernst equation relates the redox processes and the potential to the concentration/activity of the ions in the solution of an electrolytic cell. It indicates the *redox equilibrium potential V with no dc current flow*:

$$V = V_0 + (RT/nF)\ln(a_{ox}/a_{red}) \qquad \textit{The Nernst equation} \qquad (2.24)$$

Here $V_0$ is the standard electrode potential of the redox system (with respect to the hydrogen reference electrode at 1 mole concentration), $n$ is the number of electrons in the unit reaction, $R$ is not resistance but the universal gas constant, and $F$ is the Faraday constant. $a_{ox}$ and $a_{red}$ are *activities*, $a = \gamma c$, where $c$ is the concentration and $\gamma$ is the activity *coefficient*. $\gamma = 1$ for low concentrations (no ion interactions), but $< 1$ at higher concentrations. The half-cell potentials are referred to standardised conditions, meaning that the other electrode is considered to be the standard hydrogen electrode (implying the condition: pH 0, hydrogen ion activity 1 mol/L).

The Nernst equation presupposes a *reversible* reaction: that the reaction is reasonably fast in both directions. This implies that the surface concentrations of

**Table 2.10.** Standard equilibrium electrode potentials for some redox systems

| Electrode | Electrode reaction | $V_0$ (volt) |
|---|---|---|
| Pt | $2H_2O + 2e^- \rightleftharpoons H_2 + 2OH^-$ | −0.83 |
| Pt | $O_2 + 2H_2O + 2e^- \rightleftharpoons H_2O_2 + 2OH^-$ | −0.15 |
| **Pt** | $\mathbf{2H^+ + 2e^- \rightleftharpoons H_2}$ | **0** |
| Carbon | → ? | ? |
| AgCl | $AgCl + e^- \rightleftharpoons Ag + Cl^-$ | +0.22 |
| Calomel | | +0.28 |

reactants and products are maintained close to their equilibrium values. If the electrode reaction rate is slow in any direction, the concentrations at the electrode surface will not be equilibrium values, and the Nernst equation is not valid. Then the reactions are *irreversible*.

For metal cathodes the activity of the reduced forms $a_{red}$ is 1, and the equation, e.g., for an AgCl electrode is

$$V = V_{AgCl/Ag} - (RT/F) \ln a_{Cl^-} \tag{2.25}$$

where $R$ is the universal gas constant. Then the dc potential is only dependent on the activity of the $Cl^-$-anion in aqueous solution (and on temperature). The silver–silver chloride electrode is an example of an "electrode of the second kind": the electrode metal (Ag) is in equilibrium with a low-solubility salt of its ions ($Ag^+$).

**Total galvanic cell dc voltage**

According to Tables 2.9 and 2.10, two different electrode materials in the same electrolyte solution may generate one volt or more dc. Superimposed on signals in the microvolt range, this may create noise and be a problem for input amplifiers.

If both electrode surfaces are of, say, stainless steel in saline, there are not necessarily any redox reactions at the surface. The voltage is not well defined and may easily attain 100 mV or more, the system is highly polarisable and the output voltage is noisy, cf. Section 8.1. Even strongly polarisable electrode metals like stainless steel, platinum or mercury have an electrode reaction if the applied dc voltage is high enough. This is on both the anodic and cathodic side, but the reactions are irreversible and therefore not redox reactions.

Under zero-current conditions, many metal electrodes are of interest in biological work. The platinum electrode, for instance, becomes an interesting redox potential recording electrode. An inert platinum electrode may actually be used in potentiometry in the bulk of a redox system, during titration or for example in sea water analysis. With zero current the inert platinum will pick up the redox equilibrium potential of the process.

Poisson's law (eq. 7.6) defines the relationship between the potential function (representing a possible emv (electromotive voltage, Section 10.3) source to the external circuit) and the charge distribution in an electrolytic volume. A change in the charge distribution near the electrode surface results in a changed potential function, and consequently a changed half-cell potential. A polarisable electrode therefore implies a current-induced change of charge distribution near the electrode surface, and a changed half-cell potential.

**The liquid junction equilibrium dc potential**

Between two dissimilar electrolyte solutions a potential difference is created just as between a metal and an electrolytic solution. By Brownian motion the ions randomly walk with a velocity proportional to the Boltzmann factor $kT$. The corresponding $E$-field will have a direction that slows down the rapid ions and accelerates the slow ones in the interface zone. The resulting potential difference is

called the *liquid junction potential* ($\Phi_{lj}$), and follows a variant of the Nernst equation called the *Henderson* equation:

$$\Phi_{lj} = \frac{\mu^+ - \mu^-}{\mu^+ + \mu^-} \frac{RT}{nF} \ln \frac{c_1}{c_2} \tag{2.26}$$

where $R$ is the universal gas constant and $\mu^+$ and $\mu^-$ are the mobilities of cations and anions, respectively.

The liquid junction potential is usually less than 100 mV. For instance for a junction of different concentrations of NaCl and with $c_1 = 10c_2$, the dilute side is 12.2 mV negative with respect to the other side.

The $K^+$ and $Cl^-$ ions have about the same mobilities, and therefore KCl creates a lower liquid junction potential than, e.g., NaCl. The liquid junction dc potential can be kept small by inserting a *salt bridge* between the solutions, so that there will be two junctions instead of one. By using a concentrated solution of KCl in the bridge, it can be shown that the two junction potentials will tend to be equal and will be dominated by the concentrated salt solution, but with opposite sign so that they more or less cancel.

**Membrane equilibrium potentials (Donnan potential difference)**

The liquid junction potential was defined with no membrane separating the two media. A membrane separating an electrolyte in two compartments is often selectively permeable, e.g. rather open to water but less permeable to certain ions or larger charge carriers. The selectivity may be due to the mechanical dimensions of pores or to charge-dependent forces.

With different concentrations on each side, such membranes generate an osmotic pressure difference. With different ionic concentration an electrical potential difference is also generated. This is called the *Donnan potential difference*, $\Phi_D$.

$$\Phi_D = (RT/F) \ln a_1/a_2 \tag{2.27}$$

where $a_1$ is the activity of a specified ion on compartment side one, and $R$ is the universal gas constant.

### 2.5.2. The monopolar basic experiment

When we are to study electrode reactions a little further, we must be able to differentiate between cathodic and anodic processes. We therefore change the setup shown in Fig. 2.1 a little. Instead of two equal electrodes, we reduce the area of one of them to be, e.g., $< 1/100$ of the other.

With no current through the electrolytic cell, it does not matter whether the electrodes are large or small, the equilibrium potentials are the same. But with current flow, the current density and therefore the voltage drop and the polarisation, will by much higher at the small electrode. An increased potential drop will occur in the constrictional current path near the small electrode, and in general the properties of the small electrode will dominate the results. The small electrode will be the electrode studied, the *working electrode*. It is a *monopolar* system, meaning that the

effect is determined by *one* electrode. The other electrode becomes the *indifferent* or *neutral* electrode. Note that this division is not true in potentiometry; electrode area is unimportant under no-current conditions.

We let the external dc voltage change slowly (e.g. ramp voltage from a polarograph), and we record the dc current (Fig. 2.14). In electrochemistry this is called *voltammetry* (volt-am-metry), the application of a varying voltage with the measurement of current. *Ampereometry* is more generally the measurement of current with a constant amplitude voltage. *Polarography* is a form of voltammetry, preferably with the dropping mercury electrode and with a diffusion-controlled current in a monopolar system.

The solution (Fig. 2.13) is as usual NaCl 0.9% in water. With a *platinum* working electrode there will be no dc current over a rather wide voltage range (Fig. 2.14a). The *incremental* dc resistance $R = \Delta V/\Delta I$ is large in this range ($\Delta I \approx 0$). Platinum is therefore a strongly polarisable electrode material.

With a sufficiently large voltage of any polarity, dc faradaic current flows and we have an *electrode reaction* at the platinum surface. $R$ falls to smaller values. Evidently a large *activation energy* is necessary to obtain electron transfer and an electrode reaction. It is not likely that this reaction involves chemical reaction with platinum, or that platinum metal enters the solution as ions. However, in our basic experiment of Fig. 2.1 we did consider the effect of dissolved oxygen. With a suitable negative voltage, the neutral oxygen is reduced at the cathode (Fig. 2.14a, broken curve). This reaction causes a faradaic current. However, when the negative voltage is large enough, we reach a *current plateau*, again with a large incremental $R$. Then the electron transfer is no longer the rate-limiting factor, but rather the diffusion of

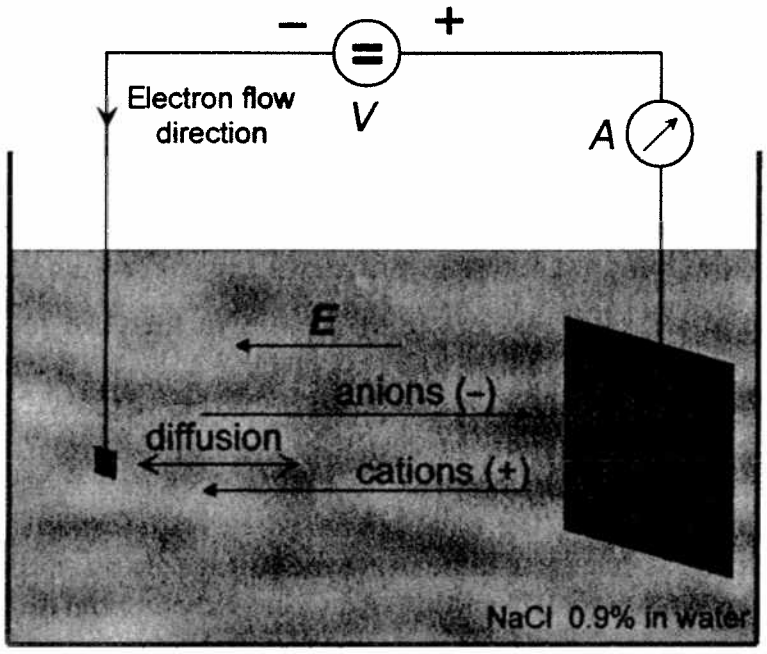


**Figure 2.13.** The basic electrolytic experiment, *monopolar* electrode system. The bipolar version is shown in Fig. 2.1.

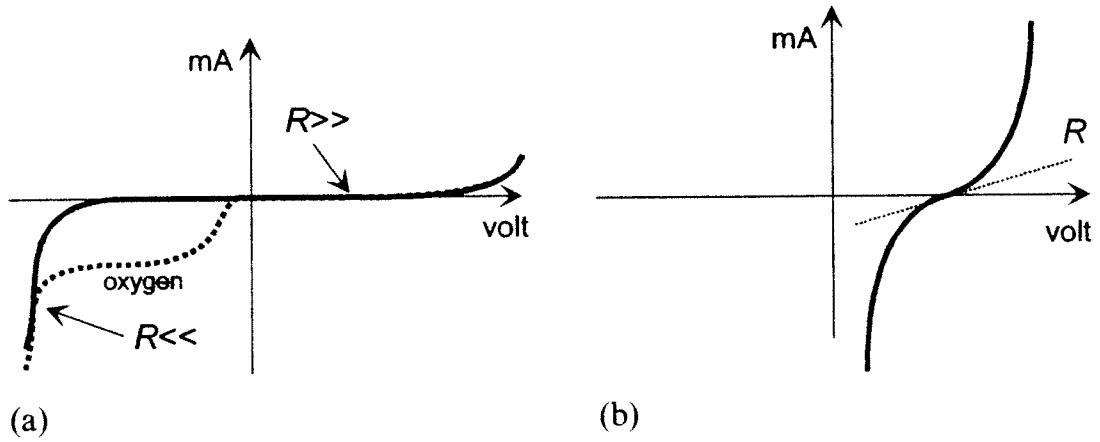


(a) (b)

**Figure 2.14.** Dc monopolar electrode current. Incremental resistance $R$ is the tangent to the curve at a given point. Working electrode (a) platinum, (b) silver–silver chloride.

oxygen to the cathode. At the cathode surface the concentration of oxygen is approximately zero; all available oxygen is reduced immediately. *The current is diffusion controlled.* The oxygen molecules are neutral in the solution and are not migrating in the electric field, they move because of the concentration gradient. At the platinum surface they are ionised (reduced), accepting electrons. This is the principle of the polarographic oxygen electrode. If we increase the voltage to about $-1.4$ volt, a much larger dc current flows, and the decomposition of water occurs with bubbles of $H_2$ appearing.

Now let us change to a small *silver/silver chloride* working electrode (Fig. 2.14b). Even with a small deviation $\Delta V$ from the equilibrium voltage with zero current, the $\Delta I$ will be large, and in either direction. Even at the equilibrium voltage, $R$ is rather small. We have an immediate, large electrode reaction. This is the non-polarisable electrode; even with relatively large dc currents the charge distribution does not change very much, neither does the dc potential. With a positive overvoltage on the electrode, the AgCl layer thickens; with a negative overvoltage it becomes thinner and is at last stripped off. Then we have changed the electrode surface to a pure silver electrode, and with a different equilibrium potential.

Suppose a small ac signal is superimposed on the dc voltage. At equilibrium dc voltage with no dc current, the ac current will flow in both directions because it is a reversible redox electrode process at the AgCl surface. With a dc current, the small ac current will be superimposed on the larger dc current and will thus change the reaction rate by only a small amount. As seen in Fig. 2.15, the resultant *ac current* will depend on the local slope of the dc current curve. The slope defines the *incremental resistance*:

$$R = \Delta V/\Delta I \tag{2.28}$$

The incremental resistance varies according to the dc (*bias*) level. As the dc current curve is not linear, it is clear that with large amplitudes the current response will not be a sine wave even if the superimposed ac voltage is a pure sine wave. Because of the

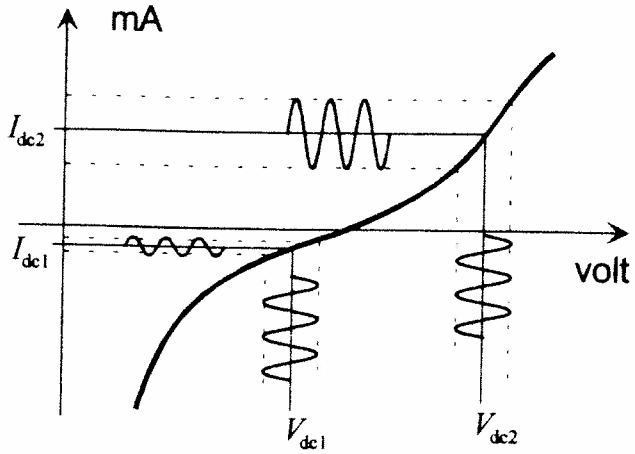


**Figure 2.15.** Superimposed ac voltage as independent variable, with dc (bias) voltage as parameter. The resulting ac current is dependent on the incremental resistance, that is the slope of the dc current curve.

capacitive properties of the cell, the current will not be in phase with the applied sine voltage.

From the curves in Fig. 2.15 it is clear that by changing the frequency and recording the ac current it is possible to examine electrode processes and find out how rapid they are. By studying the harmonic content of the current waveform as a function of dc voltage and ac amplitude/frequency, non-linearity phenomena can also be studied.

With no redox reactions, e.g. using a platinum electrode in saline, the small ac voltage will result in an ac current dependent on double layer capacitance and other components (see the next subsection).

The voltage deviation $\Delta V$ from equilibrium necessary for a certain dc current flow is called the *overvoltage*. With small deviations there is a linear relationship between $\Delta V$ and electrode current $I$, but with larger $\Delta V$ it is strongly non-linear. An overvoltage is linked with an external current and therefore the electrode is externally *polarised*.

In *cyclic voltammetry* the voltage is swept as in polarography, but at a predetermined voltage level the sweep is reversed and the cycle ends at the starting voltage. More than one cycle may be used, but usually the recorded current curve changes for each cycle. The single-cycle experiment must therefore not be confused with a steady-state ac condition. Two examples are shown in Fig. 2.16.

As the sweep is linear, the $x$-axis is both a voltage and a time axis. The charge transferred from the sweep generator to the cell is therefore proportional to the area between the curve and the $x$-axis ($=0$ mA). If the enclosed areas over and under the $x$-axis are equal, no net charge is supplied to the system. The currents may be due to double layer charging, sorption at the metal surface, or electrode reactions.

The electrolytic cell voltammograms in Fig. 2.16 are for irreversible (a) and reversible (b) processes. The irreversible process represents a net charge transfer to the cell, because very little reverse current is present. During voltage sweep a non-faradaic charge current will also flow to or from the double layer capacitance. The

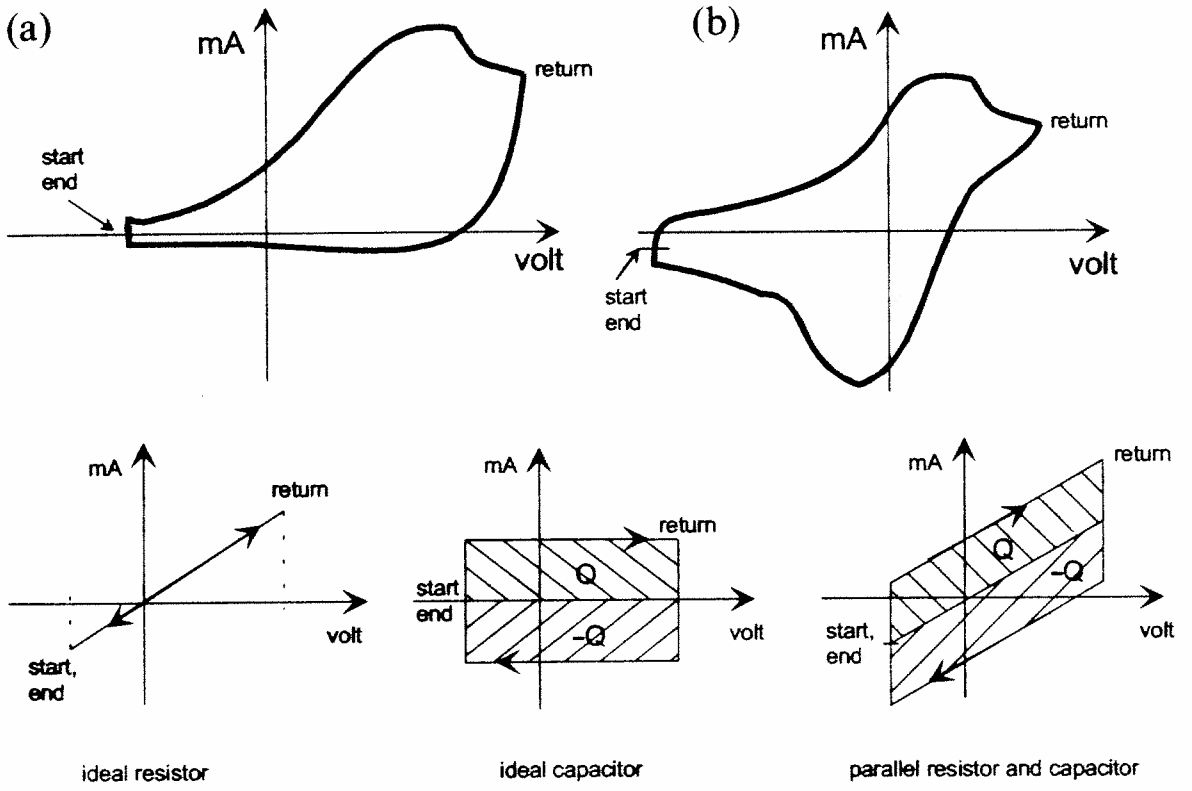


**Figure 2.16.** Cyclic voltammograms for an electrolytic cell (top): (a) irreversible reaction, (b) reversible. Bottom: with ideal components.

current steps at the sweep ends represent the reversal of such a capacitive charging current. In the reversible process most of the charge is returned—the redox reaction is reversed.

With an ideal resistor instead of the electrolytic cell (Fig. 2.16, bottom), the current curve is the same straight line, and a charge transfer equal to twice the area under the line is transferred and lost. With an ideal capacitor the charging current $I$ is $I = C\,\mathrm{d}V/\mathrm{d}t$. When $\mathrm{d}V/\mathrm{d}t$ is constant, $I$ is constant; when $\mathrm{d}V/\mathrm{d}t$ changes sign, $I$ changes sign. The area under the current curve is $Q$, and the same charge $= Q$ is returned at the return sweep. No net charge is transferred to the capacitor. The current to the parallel $RC$ components is then the sum of the separate $R$ and $C$ currents.

One type of electrode has no defined dc voltage at all: the ideally *polarisable electrode*. It can attain any potential; it is just a double-layer capacitor that can be charged to any voltage if the necessary charging current is supplied. No electron transfer occurs, no free charge carriers cross the double layer or flow in the solution. With a real electrode this implies virtually zero dc current within a certain range of applied voltage. A platinum electrode in NaCl aqueous solution is a practical example. As a current-carrying dc reference electrode in NaCl electrolyte, the platinum electrode is the worst possible choice. Another example is the dropping mercury electrode in an indifferent electrolyte, with a perfectly smooth surface continually renewed. No reversible charge transfer occurs within a rather broad range of dc voltage (oxygen-free solution).

To obtain a well-defined potential *with a variable dc current flowing*, a reversible electrochemical reaction is necessary at the electrode. Usually this implies that there must be redox reactions, with easy electron transfer in both directions. Such an electrode with easy electron transfer is called a *non-polarisable electrode*.

A redox reaction is dependent not only on the electrode material but also on the electrolyte solution. As we have seen, platinum is highly polarisable in NaCl solution. However, if the surface is saturated with dissolved hydrogen gas, a redox system is created ($H/H^+$), and then the platinum electrode becomes a *non-polarisable reference* electrode. Surface oxidation, adsorption processes and organic redox processes may reduce the polarisability and increase the applicability of a platinum electrode in tissue media.

### 2.5.3. Dc/ac equivalent circuit for electrode processes

The faradaic polarity-dependent dc currents just described are dependent not only on the applied dc voltage but also on elapsed time. With a small change in excitation voltage, it takes a certain time to reach the new current level. The four processes to be considered are:

1. A faradaic component: the rate of *electron* transfer to the electro-active species of the solution (occurring near/at the electrode surface in the double layer).
2. A faradaic component: the amount of species that can be *transported to* the reaction site from the bulk of the electrolyte, and the amount of reaction products that can be transported away *from* the reaction site.
3. The electric *charging* of the double layer.
4. The *sorption* of species at the electrode surface.

The mechanisms and speed of the *electron transfer process* have long been discussed. Does it take the electron a long time to meet the particle, or is the particle immediately ready to donate or accept an electron? When a chemical reaction is to occur, the species approach one another to a necessary close distance. In an electrode reaction, the ions enter the outer part of the double layer, and the chance increases of gaining or losing electrons. If the electroactive species are ions, what is the effect of the hydration sheath and ionic atmosphere surrounding them? Must a part of it be stripped off? The reacting partners must possess sufficient energy (translational, vibrational, rotational) to obtain reaction. The concept of necessary *activation* energy is therefore important. Sodium is very electropositive (cf. Section 2.1.1), thus tending to get rid of electrons. The most probable electrode reactions can be predicted from the electronegativity scales.

A plausible but rough electrical dc/ac equivalent circuit for the electrode processes is shown in Fig. 2.17. The electrodic part consists of three principal current paths in parallel. The elements are Cole-like as discussed in Section 7.2, and some of the component symbols used indicate that their values are non-ideal and frequency dependent.

As for the electrode processes, dc parameters are contraindicated, because a dc study should be performed with virtually zero applied overvoltage in order to be in

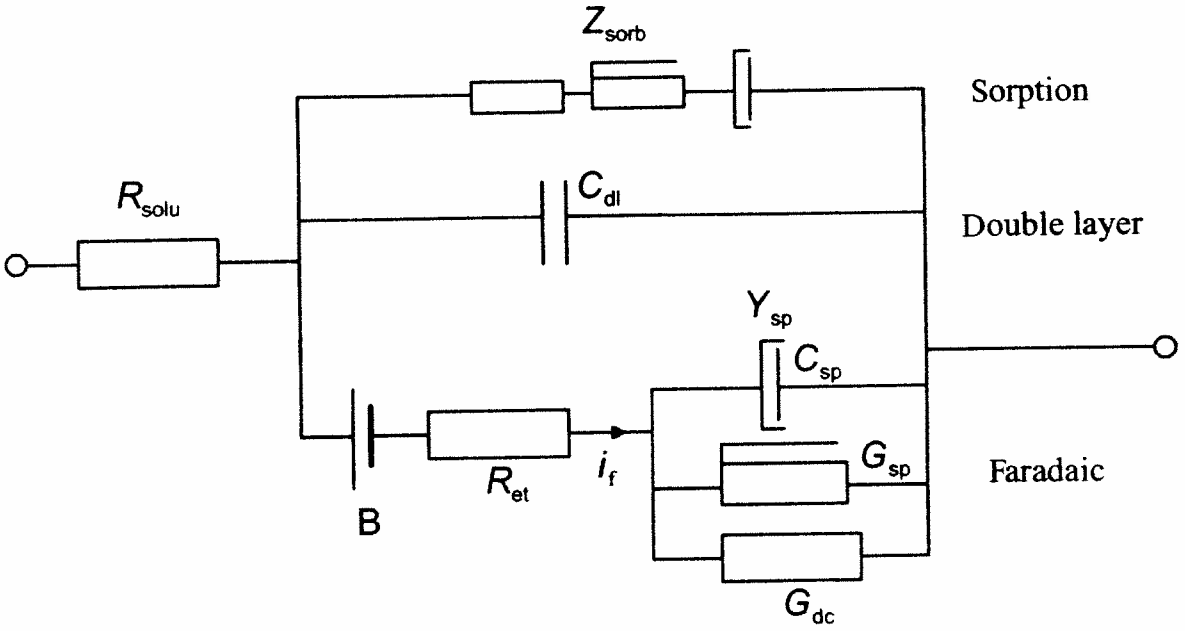


**Figure 2.17.** Electrical equivalent circuit for the three electrode processes. The subscript sp means slow processes.

the linear region (Section 6.2.1). Using a superimposed ac signal of sufficiently small amplitude with $f > 0$, the model may be a linear model, and the values of the components of the equivalent circuit may vary according to the applied dc voltage or current.

*The series resistance*

The bulk of the electrolyte obeys Ohm's law (eq. 2.2). Accordingly, the bulk electrolyte is modelled as an ideal resistor $R_{solu}$ in series with the electrode components. This is to indicate that bulk electrolytic conductance is considered frequency independent, but dependent on the geometry and possible current constrictional effects (see Fig. 5.2). If the bulk electrolyte is replaced by tissue, a more complicated equivalent circuit must replace $R_{solu}$, and we are confronted with the basic problem of division between tissue and electrode contributions.

The series resistance causes an overvoltage due to a simple $IR$-drop ($\Delta V = IR_{solu}$) in the solution. Actually this is not due to a polarisation process. However, it is often practical to include it in the total overvoltage and the electrode polarisation concept. The $IR$ drop is proportional to current, and can be reduced by the addition of a suitable strong electrolyte not intervening with the processes of interest (*indifferent* electrolyte). It can also be reduced by introducing a reference electrode reading the potential very near to the working electrode, and connecting all three electrodes to a potentiostat (see Section 5.4.1).

*1. Double layer path with leakage.* With a dripping mercury electrode the surface is ideal and the double layer is modelled as a pure, frequency-independent capacitor, somewhat voltage dependent. The capacitance values are very high because of the

small double layer thickness: $C_{dl}$ is about 20 $\mu$F/cm$^2$. With solid electrode materials the surface is of a more fractal nature, with a distribution of capacitive and resistive properties. The actual values are dependent on the type of metal, the surface conditions, the type of electrolyte and the applied voltage. The capacitance increases with higher electrolyte concentration (cf. Section 2.4.3). The double layer capacitor is inevitable, it is there as long as the metal is wetted. $C_{dl}$ may dominate the circuit if there are no sorption or electrode reaction processes.

*2. Surface sorption ac path.* The additional capacitive impedance $\mathbf{Z}_{sorb}$ is due to the adsorption and desorption of species at the electrode surface. These species do not exchange electrons with the electrode surface but they change the surface charge density and therefore cause a pure ac current path. A current-limiting resistor in series may model the processes with a Cole-like element without dc conductance (drawn as a series constant phase element because it is in series with a resistor, cf. Section 7.2.3). $\mathbf{Z}_{sorb}$ may dominate the circuit in the middle and higher Hz and lower kHz frequency ranges. Sorption currents are ac currents, and as the adsorption/desorption may occur rather abruptly at a certain dc voltage, these currents may be very dependent on the applied dc voltage. Sorption currents may dominate noble metal electrodes, so the measurement of their polarisation impedance must be performed under controlled dc voltage.

*3. Electrode reaction dc/ac path (faradaic).* The metal and the electrolyte also determine the dc half-cell potential, modelled by the battery B. If there is no electron transfer, $R_{et}$ is very large and the battery B is decoupled, the electrode is then polarisable with a poorly defined dc potential. But if there is an electrode reaction, $R_{et}$ has a lower value and connects an additional admittance in parallel with the double layer admittance. This current path is through the *faradaic impedance* $\mathbf{Z}_f$, and the current is the faradaic current $i_f$. Faradaic current is related to electrode reactions according to Faraday's law (Section 2.4.1). The faradaic impedance may dominate the equivalent circuit in the lower Hz and sub-Hz frequency ranges and at dc. The faradaic impedance is modelled by a complete Cole-like series system. It consists of the resistor $R_{et}$ modelling the electron transfer, in series with a Cole-like parallel element of *admittance* $\mathbf{Y}_{sp}$ related to slow processes (mass transport and slow electrode reactions) and therefore introducing time delays necessitating an equivalent admittance and not just a conductance.

The electron transfer resistance $R_{et}$ is related to the activation energy and to the extent to which electroactive species have reached sufficiently near the electrode surface so that acceptance or donation of electrons can occur. If the electrode voltage is not sufficient to create electron transfer and an electrode reaction, $R_{et}$ will be very large. $R_{et}$ is purely resistive, which means that there is little transfer time delay. The process is almost immediate, but energy dependent and therefore probability dependent. $R_{et}$ is clearly current dependent, and for non-polarisable electrodes it is small for all dc current values. For polarisable electrodes it is very large at zero dc current. $R_{et}$ is clearly a non-linear element. It only dominates to the

extent that electron transfer is the current-limiting process. Under that condition, the concentration of active species at the electrode is independent of current flow. Then the relationship between the *overvoltage* $\Delta V$ and the electrode current $I$ is given by the *Butler–Volmer* equation:

$$I = I_0\{\exp(\psi k\,\Delta V) - \exp[-(1-\psi)k\,\Delta V]\} \tag{2.29}$$

where $I_0$ is the exchange current present when the external current is zero, the exponent $\psi$ is called the *transfer coefficient*, and $k = zF/RT$. At equilibrium voltage with no external current, there may actually still be large reducing and oxidising local currents that cancel externally, this is $I_0$.

The slow process *admittance* $\mathbf{Y}_{sp}$ is related to reactions that are rate limited by the necessary time of transport to or from the electrode active sites, and the time of accompanying chemical reactions. If the faradaic current is limited by *diffusion alone*, the immittance is called *Warburg* immittance. $R_{et}$ is then negligible, and the current is determined by $\mathbf{Y}_{sp}$. The electron transfer flux and the chemical reaction rate are so high that the process is controlled by diffusion alone. Diffusion is a transport process dependent only on concentration gradients, cf. Section 2.4.2. The diffusion may be of reactants to the electrode, or of reaction products *away* from the electrode, both influencing $\mathbf{Y}_{sp}$. Warburg (1899) was the first to solve Fick's second law (eq. 2.10) for an electrolytic cell under ac conditions. He presumed a diffusion-controlled process with negligible migrational effects and found that under ideal conditions the concentration at the electrode surface is $+45°$ and the voltage $-45°$ out of phase with the applied current, independently of the applied frequency. Such an ideal and purely diffusion-controlled electrolytic cell is therefore a perfect model for a constant phase element (CPE). Warburg found that the concentration wave spreads out longer in the electrolyte the lower the applied frequency (Fig. 2.18).

The penetration will be delayed and can be described by a damped sine wave, so that concentrations both lower and higher than the bulk concentration may exist. It is analogous to the slow penetration of heat into a housing wall or the ground during a change in cold to warm weather. Warburg found the *diffusion zone*, defined as the distance $\delta$ from the electrode at which the concentration wave is reduced to 1/e of its value at the electrode, to be

$$\delta = (2D/\omega)^{1/2} \tag{2.30}$$

where $D$ is the diffusion constant. The diffusion zone length $\delta$ may therefore extend all the way to the countercurrent-carrying electrode at low frequencies. With $D = 10^{-9}$ m$^2$/s and at 10 $\mu$Hz, $\delta$ is 14 mm. In order to introduce negligible phase distortion, the cell length should be several centimetres long. Pure 45° properties will be found only if convection effects are negligible during the period. A purely diffusion-controlled electrode reaction has an *infinite-length Warburg admittance* with a constant (frequency-independent) phase angle $\varphi = 45°$. A more general *finite-length Warburg admittance* does not have the same constant phase character (MacDonald 1987).

The thickness of an electric double layer is about 0.1 nm with strong electrolytes,

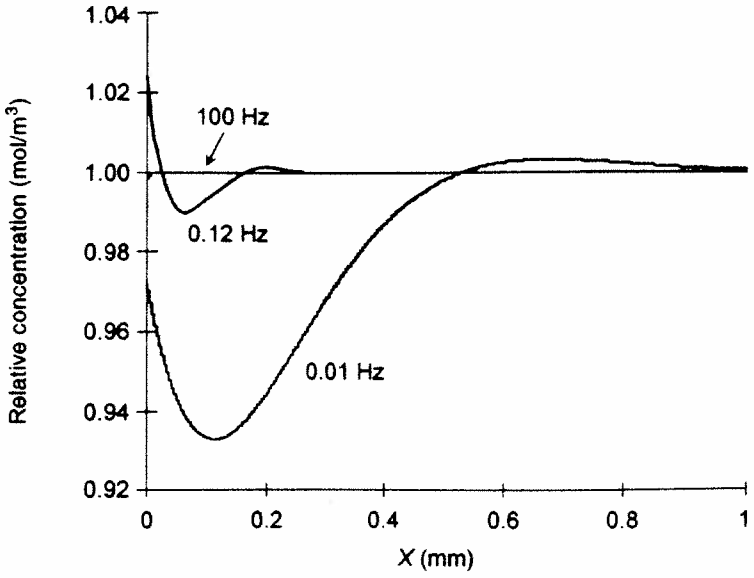


**Figure 2.18.** Ideal diffusion controlled concentration wave into the electrolyte caused by a sine wave ac current. According to Warburg (1899), his eq. 5, with the frequency of the applied current as parameter. Shown at a given moment; actually the concentration amplitude at the electrode surface will vary as a function of time according to a 45° phase-shifted sine wave. Current density and electrolyte concentration arbitrarily chosen, $D = 10^{-9}$ m$^2$/s. $X$ is the distance from the electrode surface.

about the same size as the ions, and perhaps 10 nm in dilute solutions (diffuse double layer). The thickness of a diffusion zone in unstirred solutions is enormously larger. The diffusion zone length is not dependent on concentration (as long as $D$ is constant).

The influence of the electron transfer resistor $R_{et}$ and the slow process admittance $\mathbf{Y}_{sp}$ on the total faradaic impedance is determined by which factor is reaction rate limiting. It is possible to study this by plotting the faradaic impedance as a function of frequency in a log–log plot, or in the Wessel diagram, and looking for circular arcs (see Section 7.2).

The term *electrode polarisation immittance* is sometimes related to the total immittance of the equivalent circuit of Fig. 2.17, but it is sometimes useful to exclude the series resistance $R_{solu}$ if it has the character of being an access resistance to the electrode processes. Without electrochemical reaction, measured currents are due to double layer components and sorption. The term electrode polarisation immittance should be either avoided or defined. The processes involved are of a very different nature, and in a measuring setup different variables must be controlled depending on what effects are to be studied. The electrode immittance of an electronic conductor in contact with 0.9% NaCl is of special interest to us. Data for such interfaces are found in Chapter 8.1.

### 2.5.4. Non-linear properties of electrolytics

*Electrolyte*

The bulk electrolyte solution obeys Ohm's law (eq. 2.2), which is linear. If the $E$-field changes the viscosity $\eta$ in eq. (2.6) or the number of ions per volume $n$ in eq. (2.1),

then the system is non-linear and does not obey Ohm's law (Wien 1928, Onsager 1934). This will be the case at very high electric field strengths. According to the Debye–Hückel theory, the ionic atmosphere is symmetrical about the ion in the absence of an external electric field. In an electric field the ion migrates, but its atmosphere (ionic and hydrational) is retarded by friction and is no longer symmetrical about the ion (asymmetry effect). Accordingly, at high electric fields the conductivity increases because the ions move so fast that the retarding ionic atmosphere does not have time to form: it is stripped off (the Wien[13] effect, Wien 1931).

*Electrode processes*

From Fig. 2.15 and the Butler–Volmer equation (2.29) it is clear that the dc resistance is strongly dependent on the dc current through the electrode. With an ac superimposed on a dc, the resultant ac is dependent on the incremental resistance/conductance of the dc curve. If excitation is sinusoidal, and the measured ac voltage or current also is sinusoidal, then the system is linear with the amplitudes used. On increasing the amplitude, there will be a level at which non-linearity is reached.

A dc or pulsed current polarises the electrode, and from the basic electrolytic experiment described in Section 2.2 it is also clear that faradaic current flow changes the chemical environment at the electrode surface. Current-carrying electrodes are used in such different applications as nerve stimulation, pacemaker catheter stimulation (Jaron *et al.* 1968, 1969) and defibrillation with 50 amperes passing for some milliseconds. Often a square wave pulse is used as stimulation waveform (e.g. in a pacemaker), and the necessary overvoltage is of great interest, cf. Section 8.1. In such applications a clear distinction must be made between tissue non-linearity (Section 4.4.4) and electrode non-linearity. Non-linear network theory is treated in Section 6.1.4. Non-linear behaviour in suspensions has been studied by e.g. Block and Hayes (1970) and Jones (1979); for electroporation see Section 8.12.1.

For the electrode polarisation impedance it has been shown that it was possible to state a frequency-independent *voltage* amplitude limit for linear behaviour (Onaral and Schwan 1982). This limit is about 100 mV (average, corresponding to about 300 mV p-p) ac. The corresponding *current* limit will of course be frequency dependent, and be as low as 5 $\mu$A/cm$^2$ in the lower millihertz range and as high as 100 mA/cm$^2$ in the higher kilohertz range. A typical current limit for a platinum black electrode in saline is 1 mA/cm$^2$ at 1 kHz (Schwan 1963). There is reason to believe that as the frequency approaches zero, the current limit of linearity flattens out around 5 $\mu$A/cm$^2$ where the electrode impedance becomes resistive (Onaral and Schwan 1982).

*With composite waveforms the electrode may therefore operate in the non-linear region for the low-frequency components, and in the linear region for the high-frequency components.*

[13] Wilhelm Karl Werner Wien (1864–1928), German physicist, famous for the Wien displacement law. 1911 Nobel prize laureate in physics.

The current density under a surface plate electrode is not uniform, with larger densities at the edge. The fractal properties of the electrode surface also create local areas of high current density. The onset of non-linearity may therefore be gradual, and start very early at very limited areas on the electrode surface. By harmonic analysis (Bauer 1964, Moussavi *et al.* 1994, Section 6.3.2) it has accordingly been found that very weak non-linearity is measurable at much lower voltages than 100 mV.

In a practical case when current-carrying electrodes are used with tissue, it may also be difficult to differentiate between the non-linearity of the electrode processes and the tissue processes, cf. Schwan (1992).

Electrode behaviour in the non-linear region may be studied by electrode polarisation impedance $\mathbf{Z} = R + jX$ measured as a function of sinusoidal amplitude. The limit current of linearity $i_L$ may, for instance, be defined as the amplitude when the values of $R$ or $X$ deviate more than 10% from low current density values. Often $i_L$ increases with frequency proportionally to $f^m$ (Schwan's law of non-linearity) (Onaral and Schwan 1982, McAdams and Jossinet 1991a, 1994). $m$ is the constant phase factor (as defined in this book) under the assumption that it is obeying Fricke's law and is frequency independent (Section 7.2.3). When measuring current is kept $< i_L$ they showed that Fricke's law is valid down to 10 mHz. The limit current of linearity will usually be lower for $X$ than for $R$.

### 4.3.5. Human skin and keratinised tissue

*Epithelia* are cells organised as layers: skin is an example. Cells in epithelia form *gap junctions*. In particularly tight membranes these junctions are special *tight junctions*. The transmembrane admittance is dependent both on the type of cell junction and to what extent the epithelium is shunted by channels or specialised organs (e.g. sweat ducts in the skin).

The impedance of the skin is dominated by the stratum corneum at low frequencies. It has generally been stated that skin impedance is determined mainly by the stratum corneum at frequencies below 10 kHz and by the viable skin at higher frequencies (Ackmann and Seitz 1984). This will of course be dependent on factors such as skin hydration, electrode size and geometry, but may nevertheless serve as a rough guideline. A finite element simulation of a concentric two-electrode system used by Yamamoto *et al.* (1986) showed that the stratum corneum accounted for about 50% of the measured skin impedance at 10 kHz, but only about 10% at 100 kHz (Martinsen *et al.* 1999).

The stratum corneum (SC) may have a thickness of from about 10 $\mu$m (0.01 mm) to as much as 1 mm or more, e.g. on the sole of the foot. It is a solid-state substance, not necessarily containing liquid water, but with a moisture content dependent on the surrounding air humidity. SC is not soluble in water, but the surface will be charged and a double layer will be formed in the water side of the interphase. SC can absorb large amounts of water, for example doubling its weight. It may be considered as a solid-state electrolyte, perhaps with few ions free to move and contribute to dc conductance. The SC contains such organic substances as proteins and lipids, which may be highly charged but bound, and therefore contribute only to ac admittance.

An open question is whether the conductance in SC, in addition to the ionic component, also has an electronic component, e.g. as a semiconductor.

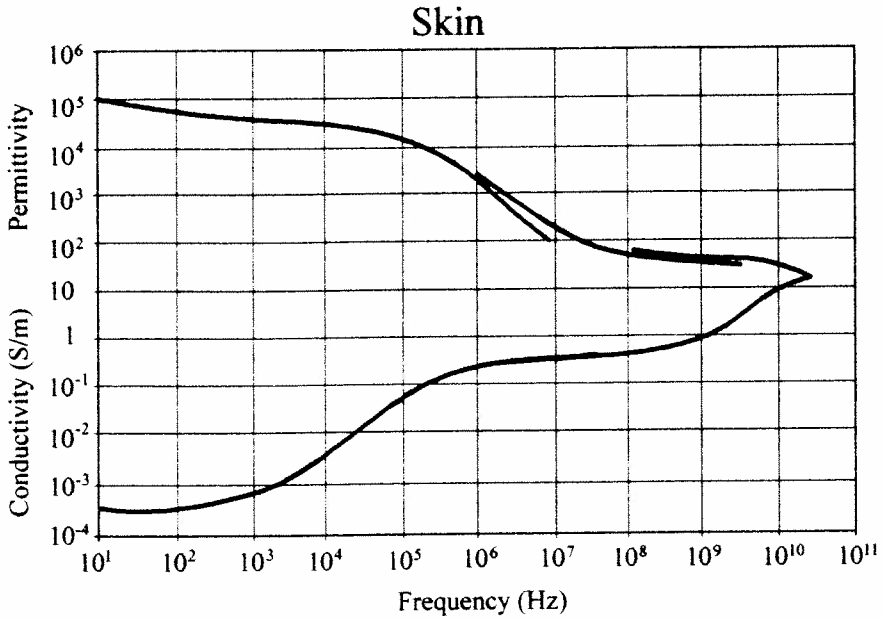


**Figure 4.19.** Dielectric dispersion of skin tissue. Based on Gabriel *et al.* (1996), by permission.

The stratum corneum has been shown to display a very broad $\alpha$-dispersion (Figs 4.19 and 4.20) that is presumably largely due to counterions. Viable skin has electrical properties that resemble those of other living tissue, and hence displays separate $\alpha$- and $\beta$-dispersions. The interface between the SC and the viable skin will also give rise to a Maxwell–Wagner type of dispersion in the $\beta$-range. While the impedance of the SC is much higher at low frequencies than the impedance of the living skin, the differences in dispersion mechanisms make the electrical properties converge as the frequency is increased. This is the main reason why increased frequency in general leads to measurements of deeper layers in the skin.

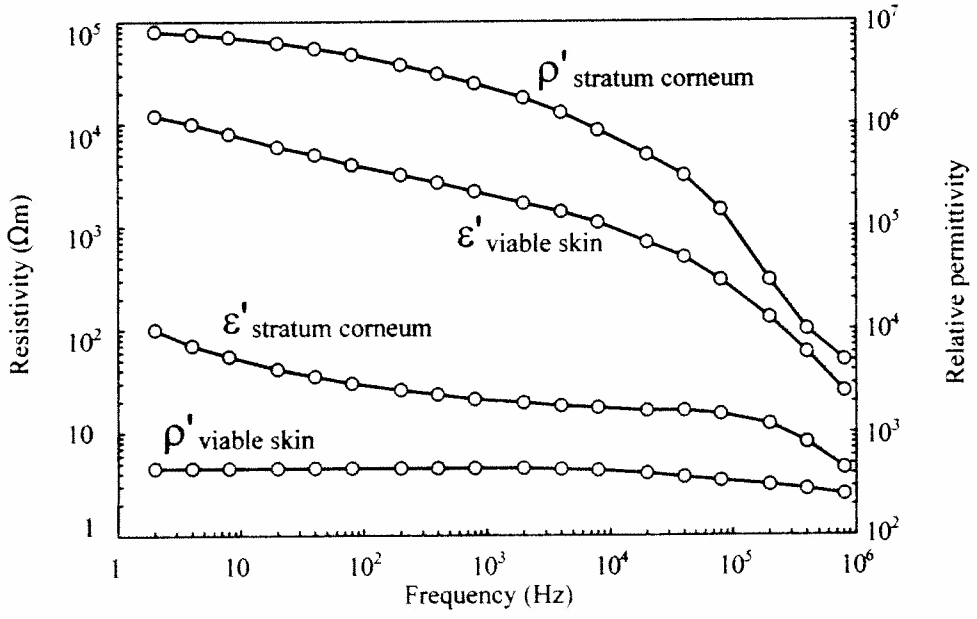


**Figure 4.20.** Average resistivities and relative permittivities in stratum corneum and viable skin. Redrawn from Yamamoto and Yamamoto (1976), by permission.

Yamamoto and Yamamoto (1976) measured skin impedance on the ventral side of the forearm with a two-electrode system and an ac bridge. They used Beckman Ag/AgCl electrodes filled with gel and measured 30 min after the electrodes had been applied. The skin was stripped with cellulose tape 15 times, after which the entire SC was believed to have been removed. Impedance measurements were also carried out between each stripping so that the impedance of the removed layers could be calculated. The thickness of the SC was found to be 40 $\mu$m, which is more than common average values found elsewhere in the literature. Therkildsen *et al.* (1998), for example, found a mean thickness of 13.3 $\mu$m (min. 8 $\mu$m/max. 22 $\mu$m) when analysing 57 samples from non-friction skin sites on caucasian volunteers. However, the increase in moisture caused by electrode occlusion and electrode gel would certainly have increased the stratum corneum thickness significantly.

Knowing the stratum corneum thickness enabled Yamamoto *et al.* to calculate the parallel resistivity and relative permittivity of the removed stratum corneum. Furthermore, the resistivity and relative permittivity of the viable skin were calculated by assuming homogeneous electrical properties and using the formula for the constrictional resistance (cf. Fig. 5.2). The resistance of a disk surface electrode is (eq. 5.9): $R = \rho/4a$. Since $RC = \rho\varepsilon_r\varepsilon_0$, the relative permittivity of the viable skin can be calculated from the measured capacitance using the formula: $C = 4a\varepsilon_r\varepsilon_0$. The calculated data from Yamamoto and Yamamoto (1976) are presented in Fig. 4.20. These data can also be presented as conductance and susceptance versus frequency as in Fig. 4.21. The very broad nature of the dispersion can easily be seen in this figure. The conductance levels out at low frequencies, indicating the dc conductance level of the skin. The susceptance seems to reach a maximum at approximately 1 MHz, which should then correspond to the characteristic frequency of the dispersion. This frequency response is difficult to interpret and the apparent broad dispersion is most probably a composite of several dispersion

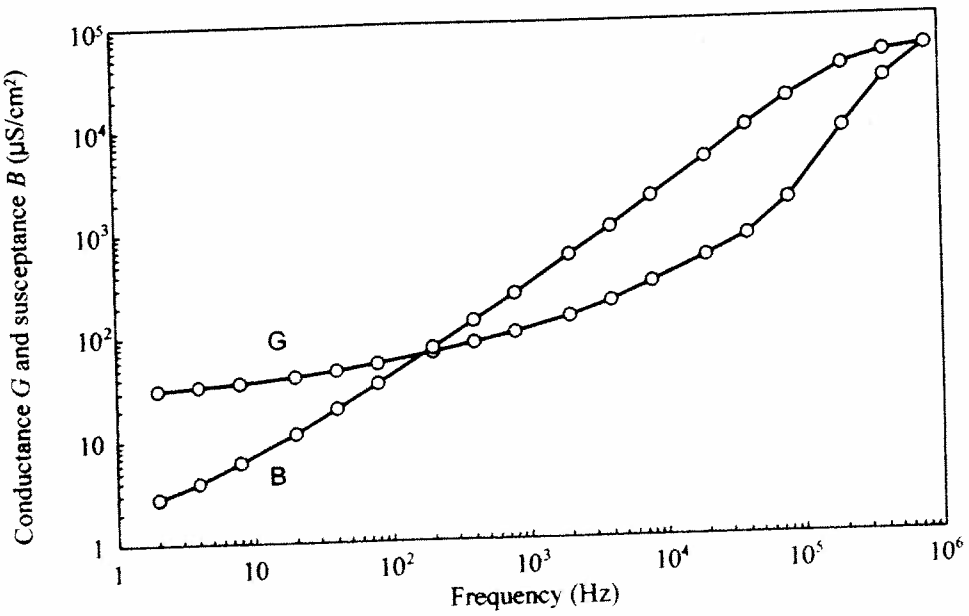


**Figure 4.21.** Electrical admittance of the stratum corneum as calculated from data presented in Fig. 4.20.

mechanisms. The highly inhomogeneous nature of the stratum corneum with a significant hydration gradient in brick-like layers of dead, keratinised cells should produce significant dispersion mechanisms in both the alpha and beta ranges.

The frequency response shown in Fig. 4.21 can be compared with the admittance data from a 180 $\mu$m thick sample of palmar stratum corneum *in vitro* shown in Fig. 4.22 (Martinsen *et al.* 1997a). These measurements were performed with a two-electrode system and hydrogel electrodes at 50% relative humidity. The dc level of this stratum corneum sample is much lower than that shown in Fig. 4.21, even after adjusting for the 4.5 times greater thickness of the *in vitro* sample. This is easily explained from the difference in hydration for the two samples. Stratum corneum *in situ* is hydrated by the underlying viable skin and, in this case, also by the electrode gel. The *in vitro* skin is in balance with the ambient relative humidity and the hydrogel electrodes do not increase the hydration (Jossinet and McAdams 1991).

An important finding by Yamamoto and Yamamoto (1976) was that the impedance of the removed stratum corneum layers did not produce a circular arc in the complex impedance plane. This is obvious from Fig. 4.23, where the admittance data from Fig. 4.21 have been transformed to impedance values and plotted in the complex plane. Hence, if one plots the data from multi-frequency measurements on skin *in vivo* in the complex plane and uses a circular regression in order to derive, e.g., the Cole parameters, one must be aware that stratum corneum alone does not necessarily produce a circular arc, and as described earlier in this chapter, the measured volume or skin layer is highly dependent on frequency. The derived parameters therefore represent a mixture of different skin layers and different dispersion mechanisms and are thus totally ambiguous when used for characterising conditions of specific skin layers.

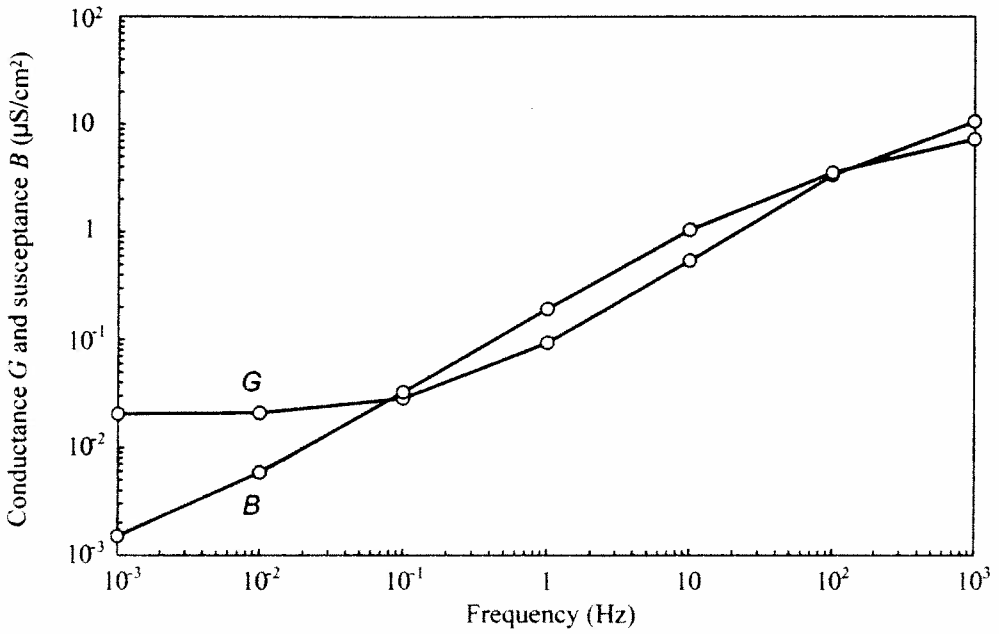


**Figure 4.22.** Electrical admittance of palmar stratum corneum *in vitro*. Martinsen *et al.* (1997a), by permission.

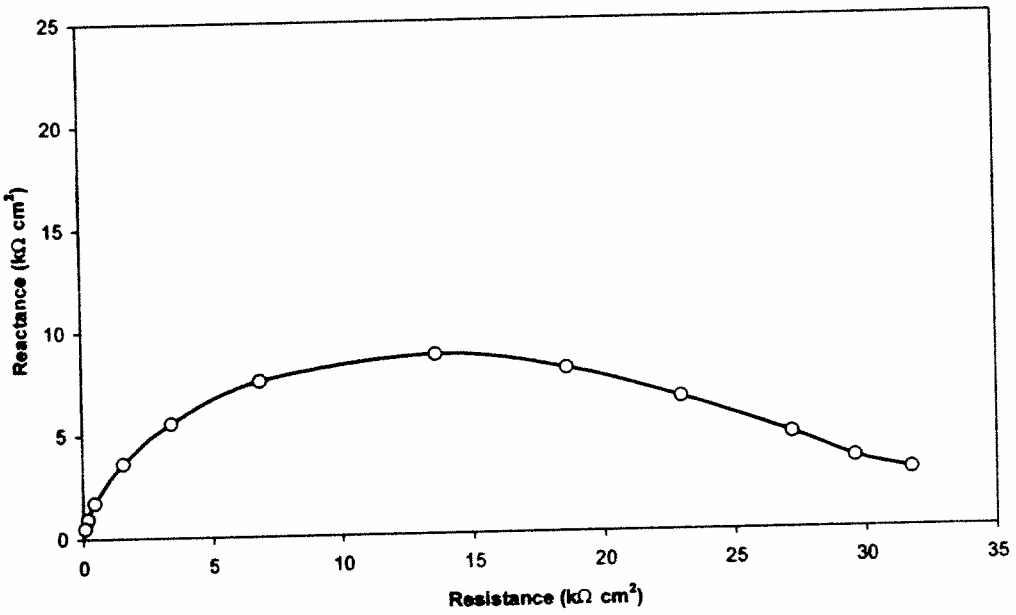


**Figure 4.23.** The stratum corneum data from Fig. 4.21 plotted in the complex impedance plane.

Skin admittance varies greatly both between persons and between different skin sites on the same person. Changes in, for example, sweat gland activity and ambient relative humidity during the day or year season are also reflected in large variations in skin admittance, mainly because of changes in skin hydration.

Table 4.2 shows the results from impedance measurements at 10 Hz on different skin sites as measured with a 12 $cm^2$ dry metal ECG plate electrode positioned directly on the skin site after a short breath had been applied to the skin surface (Grimnes 1983a) in order to create a surface film of water molecules for improved

**Table 4.2.** Site dependence of skin impedance (k$\Omega$ $cm^2$) at 10 Hz, dry electrode plate. Initial values and values obtained after two intervals of 2 hours. Each measurement is compared with the value (k$\Omega$) obtained from a control pre-gelled 12 $cm^2$ ECG electrode on the ventral forearm. Reproduced from Grimnes (1983a)

| | k$\Omega$ $cm^2$/k$\Omega$ | | |
|---|---|---|---|
| | Start | 2 hours | 4 hours |
| Hand: dorsal side | 720/80 | 210/17 | 300/33 |
| Forearm: ventral–distal | 250/80 | 240/17 | 190/35 |
| Forearm: ventral–middle | 840/80 | 230/17 | 360/36 |
| Forearm: ventral–proximal | 560/80 | 180/17 | 260/36 |
| Upper arm: dorsal | 840/75 | 260/16 | 660/36 |
| Upper arm: ventral | 1000/70 | 300/16 | 780/34 |
| Forehead | 60/70 | 36/16 | 48/35 |
| Calf | 325/45 | 375/17 | 325/36 |
| Thorax | 130/37 | 110/16 | 130/35 |
| Palm | 200/80 | 150/17 | 200/33 |
| Heel | 120/60 | 180/15 | 120/35 |

skin–metal electrolytic contact. The first column presents measurements immediately after the electrode had been applied, and the two subsequent columns gives the values after 2 and 4 hours respectively. The dry measuring plate electrode was removed immediately after each measurement. The first column shows a large variation in the control impedance, which was interpreted as unstable filling of sweat ducts during the measurement. The two other columns show stable results at two different levels of control. The values in Table 4.2 clearly demonstrate the large variability in skin impedance on different skin sites, and how this changes during a period of skin occlusion.

The sweat ducts of the skin introduce electrical shunt paths for dc current. Although lateral counterion relaxation effects have been demonstrated in pores, this effect is presumably negligible in sweat ducts, and sweat ducts are hence predominantly conductive (Martinsen *et al.* 1998). The dc conductance measured on human skin is not only due to the sweat ducts, however. Measurements on isolated stratum corneum as well as nail and hair reveal conductance values comparable to those found on skin *in vivo* (Martinsen *et al.* 1997a,b).

Since sweat duct polarisation is insignificant, the polarisation admittance of the skin is linked to the stratum corneum alone. This implies that measurements of capacitance or ac conductance at low frequencies reflect only the properties of the stratum corneum.

The series resistance, i.e. the limiting impedance value at very high frequencies, is very small for the stratum corneum. In a practical experimental setup, the impedance of the viable skin will in fact overrule this component. The value of this effective series resistance is typically in the range 100–500 Ω.

**Skin penetrated by external electrolytes**

In low-frequency applications, < 100 Hz, the skin impedance is very high compared to the polarisation impedance of wet electrodes and deeper tissue impedance. The stratum corneum consists of dead and dry tissue, and its admittance is very dependent on the state of the superficial layers and the water content (humidity) of the surrounding air in contact with the skin prior to electrode application. In addition, the sweat ducts shunt the stratum corneum with a very variable dc conductance. Sweat both fills the ducts and moisturises the surrounding stratum corneum. The state of the skin and measured skin admittance at the time of electrode application is therefore very variable. With low sweat activity and dry surroundings, the skin admittance may easily attain values < 1 $\mu S/cm^2$ at 1 Hz.

From the time of application of a *dry* metal plate, the water from the deeper, living layers of the skin will slowly build up both a water contact with the initially dry plate and water content in the stratum corneum. A similar process will take place in the skin with hydrogel as contact medium (but here the metal/gel interphase is already established). The processes may take a quarter of an hour or more. The water vapour pressure of the hydrogel may be such as to supply or deplete the stratum corneum of water, depending on the initial skin conditions.

To avoid a long period of poor contact, a skin drilling technique may remove the stratum corneum. Even mild rubbing with sandpaper may reduce the initial

impedance considerably. To shorten the long period of poor contact, an electrolytic solution or wet gel is often applied to the skin. The electrolyte concentration of the contact medium is very important. With high salt concentration, the water osmotic pressure in the deeper layers will strongly increase the water transport up through the skin to the high-concentration zone. This may be admissible for short-time use (e.g. $< \frac{1}{2}$ hour). For prolonged use, skin irritation may be intolerable. For long-term use, the concentration must be reduced to the range of a physiological saline solution (around 1% of electrolytes by weight).

A surface electrode with contact electrolyte covering a part of the skin may influence measured skin immittance by four different mechanisms:

1. Changing the water partial pressure gradient in the stratum corneum (SC).
2. Osmotic transport of water to or from the contact electrolyte.
3. Penetration of substances from the electrode gel into the SC.
4. Changing the sweat duct filling.

With a dry electrode plate, the moisture buildup and increase in admittance in the SC start at the moment of electrode application. With a hydrogel, admittance may increase or decrease. With wet gel or a liquid the initial admittance is high, and with strong contact electrolytes the admittance will further increase for many hours and days (Fig. 4.24). As the outer layers of stratum corneum may be wet or dry according to the humidity of the ambient air, it will not be possible to find a general contact medium that just stabilises the water content in the state it was in before electrode application, and the onset of the electrode will generally influence the parameters measured.

With dry skin the admittance may be $< 1\ \mu S/cm^2$ at 1 Hz. A typical admittance of $> 100\ \mu S/cm^2$ is possible when the stratum corneum is saturated by electrolytes and water. The conductivity is very dependent on water content and is believed to be

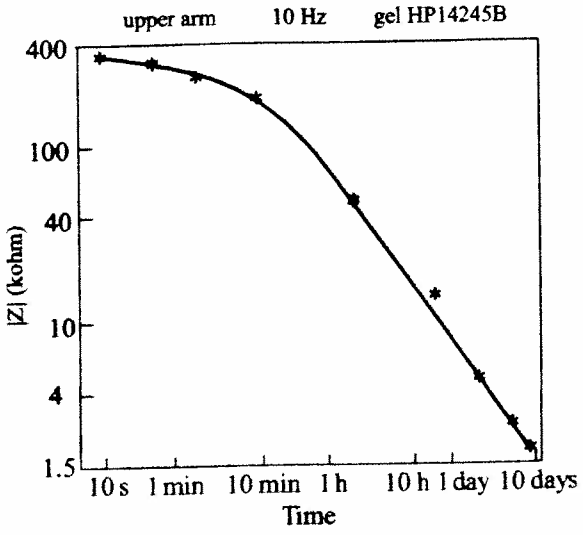


**Figure 4.24.** Skin impedance as a function of time with an ECG electrode of commercial, wet gel, strong electrolyte type. From Grimnes (1983a), by permission.

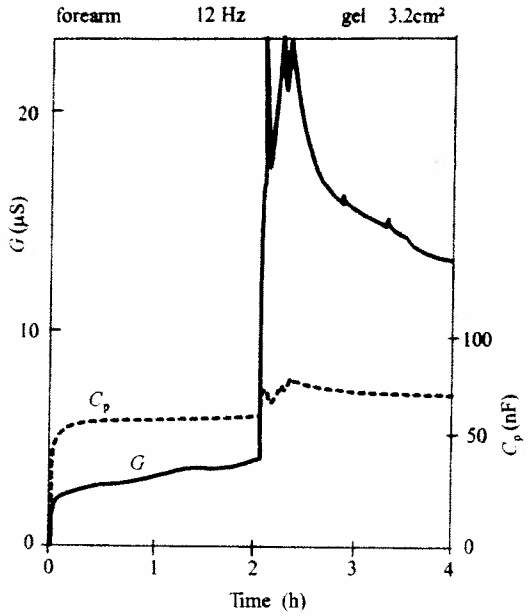


**Figure 4.25.** *In vivo* skin conductance and parallel capacitance during abrupt sweat duct filling (sudden physical exercise) and emptying. From Grimnes (1984), by permission.

caused, for example, by ions, protons ($H^+$) and charged, bound proteins that contribute only to ac-admittance.

Figure 4.25 shows the dominating effect of sweat duct filling on skin admittance, and shows clearly how skin capacitance is in parallel and therefore unaffected by the parallel conductance change.

# MEDICAL INSTRUMENTATION
## Application and Design

SECOND EDITION

**John G. Webster, Editor**

Contributing Authors

**John W. Clark, Jr.**
Rice University

**Michael R. Neuman**
Case Western Reserve University

**Walter H. Olson**
Medtronic, Inc.

**Robert A. Peura**
Worcester Polytechnic Institute

**Frank P. Primiano, Jr.**
Technidyne, Inc.

**Melvin P. Siedband**
University of Wisconsin–Madison

**John G. Webster**
University of Wisconsin–Madison

**Lawrence A. Wheeler**
Little Company of Mary Hospital

HOUGHTON MIFFLIN COMPANY BOSTON TORONTO
Dallas ♦ Geneva, Illinois ♦ Palo Alto ♦ Princeton, New Jersey

## 6.2 THE ELECTROCARDIOGRAPH

To learn more about biopotential amplifiers, we shall examine a typical clinical electrocardiograph. First, let us review the ECG itself.

### THE ECG

As we learned in Section 4.6, the beating heart generates an electric signal that can be used as a diagnostic tool for examining some of the functions of the heart. This electric activity of the heart can be approximately represented as a vector quantity. Thus we need to know the location at which signals are detected, as well as the time-dependence of the amplitude of the signals. Electrocardiographers have developed a simple model to represent the electric activity of the heart. In this model, the heart consists of an electric dipole located in the partially conducting medium of the thorax. Figure 6.1 shows a typical example.

This particular field and the dipole that produces it represent the electric activity of the heart at a specific instant. At the next instant the dipole can change its magnitude and its orientation, thereby causing a change in the electric field. Once we accept this model (it is an oversimplification), we need not draw a field plot every time we want to discuss the dipole field of the heart. Instead, we can represent it by its dipole moment, a vector directed from the negative charge to the positive charge and having a

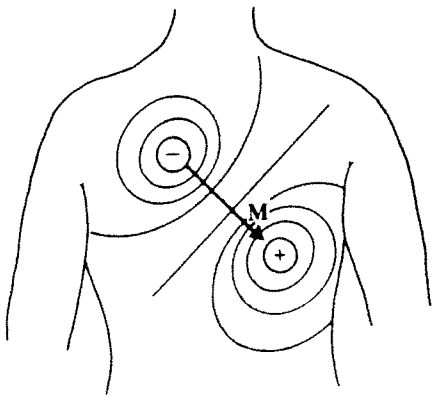


**Figure 6.1 Rough sketch of the dipole field of the heart when the R wave is maximal** The dipole consists of the points of equal positive and negative charge separated from one another and denoted by the dipole moment vector **M**.

magnitude proportional to the amount of charge (either positive or negative) multiplied by the separation of the two charges. In electrocardiography this dipole moment, known as the *cardiac vector*, is represented by **M**, as shown in Figure 6.1. As we progress through a cardiac cycle, the magnitude and direction of **M** vary because the dipole field varies.

The electric potentials generated by the heart appear throughout the body and on its surface. We determine potential differences by placing electrodes on the surface of the body and measuring the voltage between them, being careful to draw little current (ideally there should be no current at all, because current distorts the electric field that produces the potential differences). If the two electrodes are located on different equal-potential lines of the electric field of the heart, a nonzero potential difference is measured. Different pairs of electrodes at different locations generally yield different results because of the spatial dependence of the electric field of the heart. Thus it is important to have certain standard positions for clinical evaluation of the ECG. The limbs make fine guideposts for locating the ECG electrodes. We shall look at this in more detail later.

In the simplified dipole model of the heart, it would be convenient if we could predict the voltage, or at least its waveform, in a particular set of electrodes at a particular instant of time when the cardiac vector is known. We can do this if we define a *lead vector* for the pair of electrodes. This vector is a unit vector that defines the direction a constant-magnitude cardiac vector must have to generate maximal voltage in the particular pair of electrodes. A pair of electrodes, or combination of several electrodes through a resistive network that gives an equivalent pair, is referred to as a *lead*.

For a cardiac vector **M**, as shown in Figure 6.2, the voltage induced in a lead represented by the lead vector $\mathbf{a}_1$ is given by the component of **M** in the direction of $\mathbf{a}_1$. In vector algebra, this can be denoted by the dot product

$$v_{a1} = \mathbf{M} \cdot \mathbf{a}_1 \tag{6.1}$$

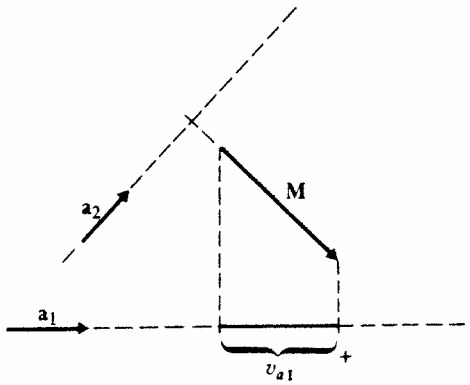


**Figure 6.2** Relationships between the two lead vectors $\mathbf{a}_1$ and $\mathbf{a}_2$ and the cardiac vector **M**. The component of **M** in the direction of $\mathbf{a}_1$ is given by the dot product of these two vectors and denoted on the figure by $v_{a1}$. Lead vector $\mathbf{a}_2$ is perpendicular to cardiac vector, so no voltage component is seen in this lead.

where $v_{a1}$ is the scalar voltage seen in the lead that has the vector $\mathbf{a}_1$. Let us consider another lead, represented by the lead vector $\mathbf{a}_2$, as seen in Figure 6.2. In this case, the vector is oriented in space so as to be perpendicular to the cardiac vector **M**. The component of **M** along the direction of $\mathbf{a}_2$ is zero, so no voltage is seen in this lead as a result of the cardiac vector. If we measured the ECG generated by **M** using one of the two leads shown in Figure 6.2 alone, we could not describe the cardiac vector uniquely. However, by using two leads with different lead vectors, both of which lie in the same plane as the cardiac vector, we can describe **M**.

In clinical electrocardiography, more than one lead must be recorded to describe the heart's electric activity fully. In practice, several leads are taken in the *frontal plane* (the plane of your body that is parallel to the ground when you are lying on your back) and the *transverse plane* (the plane of your body that is parallel to the ground when you are standing erect).

Three basic leads make up the *frontal-plane* ECG. These are derived from the various permutations of pairs of electrodes when one electrode is located on the right arm (RA in Figure 6.3), the left arm (LA), and the left leg (LL). Very often an electrode is also placed on the right leg (RL) and grounded or connected to special circuits, as shown in Figure 6.19. The resulting three leads are lead I, LA to RA; lead II, LL to RA; and lead III, LL to LA. The lead vectors that are formed can be approximated as an equilateral triangle, known as *Eindhoven's triangle*, in the frontal plane of the body, as shown in Figure 6.3. Because the scalar signal on each lead of Eindhoven's triangle can be represented as a voltage source, we can write Kirchhoff's voltage law for the three leads.

$$\mathrm{I} - \mathrm{II} + \mathrm{III} = 0 \tag{6.2}$$

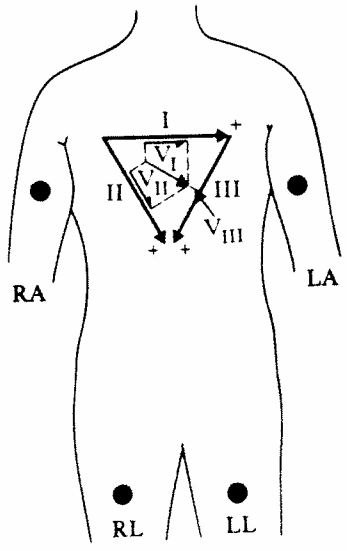


**Figure 6.3** Cardiologists use a standard notation such that the direction of the lead vector for lead I is 0°, that of lead II is 60°, and that of lead III is 120°. An example of a cardiac vector at 30° with its scalar components seen for each lead is shown.

The components of a particular cardiac vector can be determined easily by placing the vector within the triangle and determining its components along each side. The process can also be reversed, which enables us to determine the cardiac vector when we know the components along the three lead vectors, or at least two of them. It is this latter problem that usually concerns the electrocardiographer.

Three additional leads in the frontal plane—as well as a group of leads in the transverse plane—are routinely used in taking clinical ECGs. These leads are based on signals obtained from more than one pair of electrodes. They are often referred to as *unipolar leads*, because they consist of the potential appearing on one electrode taken with respect to an equivalent reference electrode, which is the average of the signals seen at two or more electrodes.

One such equivalent reference electrode is the *Wilson central terminal*, shown in Figure 6.4. Here the three-limb electrodes just described are connected through equal-valued resistors to a common node. The voltage at this node, which is the Wilson central terminal, is the average of the voltages at each electrode. In practice, the values of the resistors should be at least 5 MΩ so that the loading of any particular lead will be minimal. Thus, a more practical approach is to use buffers (voltage followers, see

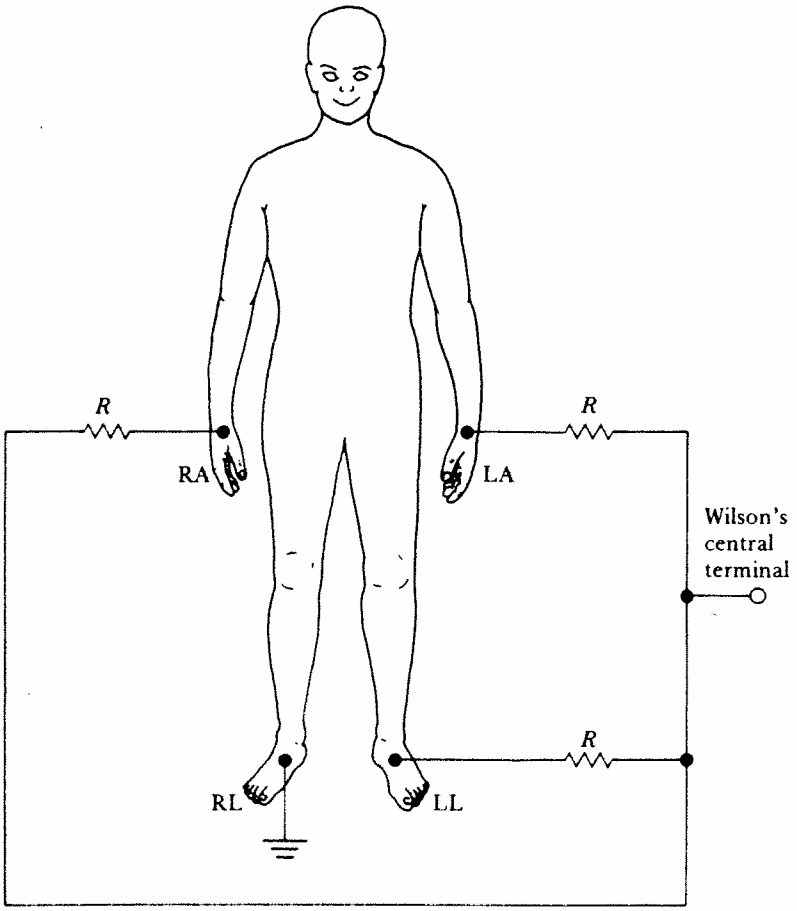


**Figure 6.4** Connection of electrodes to the body to obtain Wilson's central terminal

Section 3.3) between each electrode and the equal-valued resistors. The signal between LA and the central point is known as VL, that at RA as VR, and that at the left foot as VF. Note that for each of these leads, one of the resistances $R$ shunts the circuit between the central terminal and the limb electrode. This tends to reduce the amplitude of the signal observed, and we can modify these leads to *augmented leads* by removing the connection between the limb being measured and the central terminal. This does not affect the direction of the lead vector but results in a 50% increase in amplitude of the signal.

The augmented leads—known as aVL, aVR, and aVF—are illustrated in Figure 6.5, which also illustrates their lead vectors, along with those of leads I, II, and III. Note that when the negative direction for aVR is considered with the other five, all six vectors are equally spaced, by 30°. It is thus possible for the cardiologist looking at an ECG consisting of these six leads to estimate the position of the cardiac cycle by seeing which of the six leads has the greatest signal amplitude at that point in the cycle.

When physicians look at the ECG in the transverse plane, they use *precordial* (chest) leads. They place an electrode at various anatomically defined positions on the chest wall, as shown in Figure 6.6. The potential between this electrode and Wilson's central terminal is the electrocardiogram for that particular lead. Figure 6.6 also shows the lead-vector positions. Physicians can obtain ECGs from the posterior side of the heart by means of an electrode placed in the esophagus. This structure passes directly behind the heart, and the potential between the esophageal electrode and Wilson's central terminal gives a posterior lead.

**EXAMPLE 6.1** Show that the voltage in lead aVR is 50% greater than that in lead VR at the same instant.

**ANSWER** Considering the connections for aVR and VR, we can draw the equivalent circuits of Figure E6.1. The voltages between each limb and ground are $v_a$, $v_b$, and $v_c$. When no current is drawn by the voltage-measurement circuit, the negative terminal for aVR (the modified Wilson's central terminal) is at a voltage of $v'_w$ with respect to ground, which can be determined as follows:

$$i_1 = \frac{v_b - v_c}{2R}$$

$$v'_w = i_1 R + v_c = \frac{v_b - v_c}{2R} R + v_c = \frac{v_b + v_c}{2} \tag{E6.1}$$

Because no current is drawn, the positive aVR terminal (RA) is at a voltage $v_a$ with respect to ground. Then aVR is

$$\text{aVR} = v_a - \frac{v_b + v_c}{2} = \frac{2v_a - v_b - v_c}{2} \tag{E6.2}$$

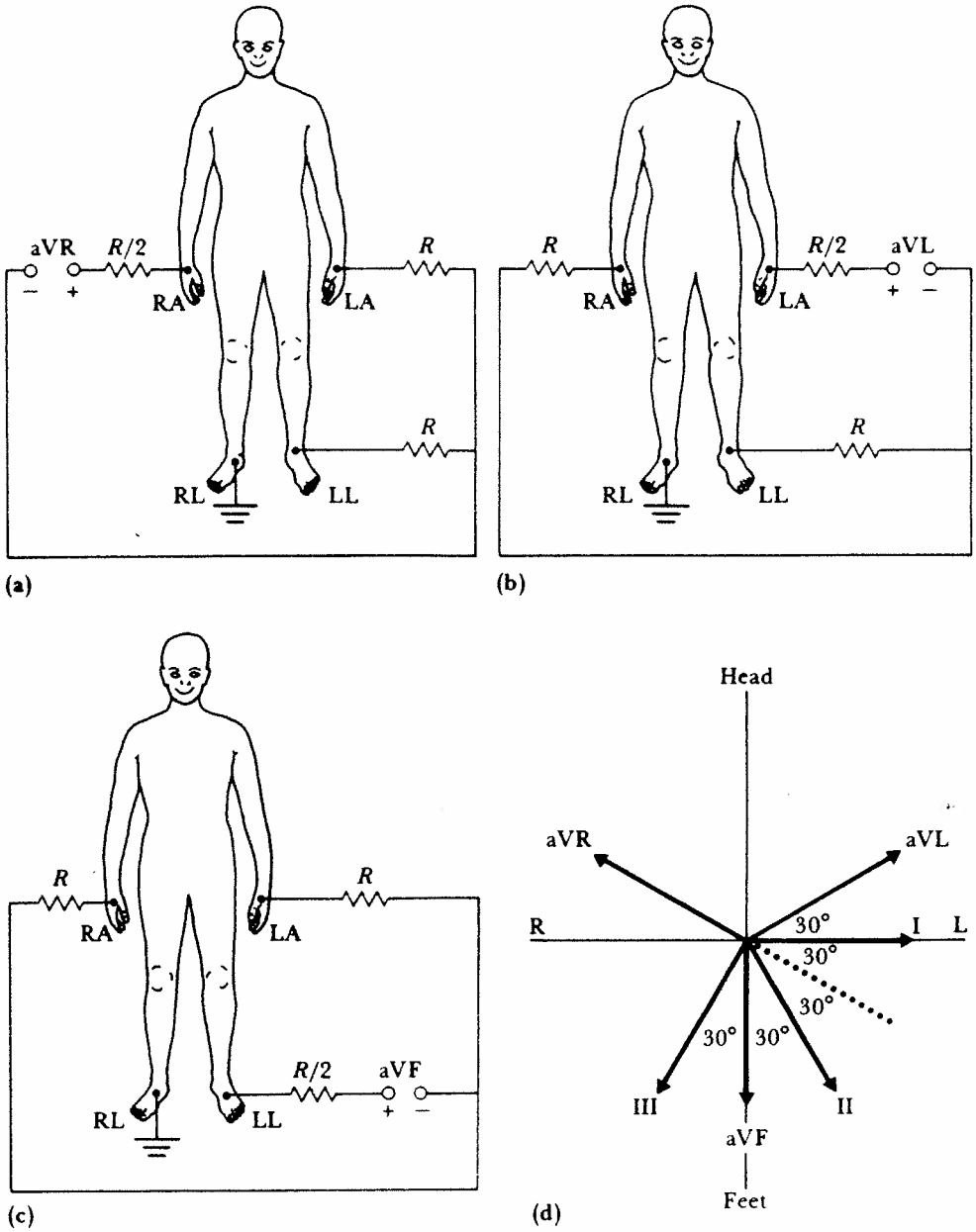


**Figure 6.5** (a), (b), (c) Connections of electrodes for the three augmented limb leads. (d) Vector diagram showing standard and augmented lead-vector directions in the frontal plane.

We can determine VR from Figure E6.1(b). To find the Wilson's central terminal voltage $v_w$, we simplify the circuit by taking the Thévenin equivalent circuit of the two right-hand branches. This gives the circuit shown in Figure E6.2, where $v'_w$ comes from (E6.1). Now $v_w$ is

$$v_w = \frac{v_a - v'_w}{3R/2}\frac{R}{2} + v'_w = \frac{v_a + 2v'_w}{3} \tag{E6.3}$$

$$v_w = \frac{v_a + 2(v_b + v_c)/2}{3} = \frac{v_a + v_b + v_c}{3} \tag{E6.4}$$

Thus

$$\mathrm{VR} = v_a - v_w = \frac{2v_a - v_b - v_c}{3} \tag{E6.5}$$

which shows that

$$\mathrm{aVR} = \tfrac{3}{2}\mathrm{VR}$$

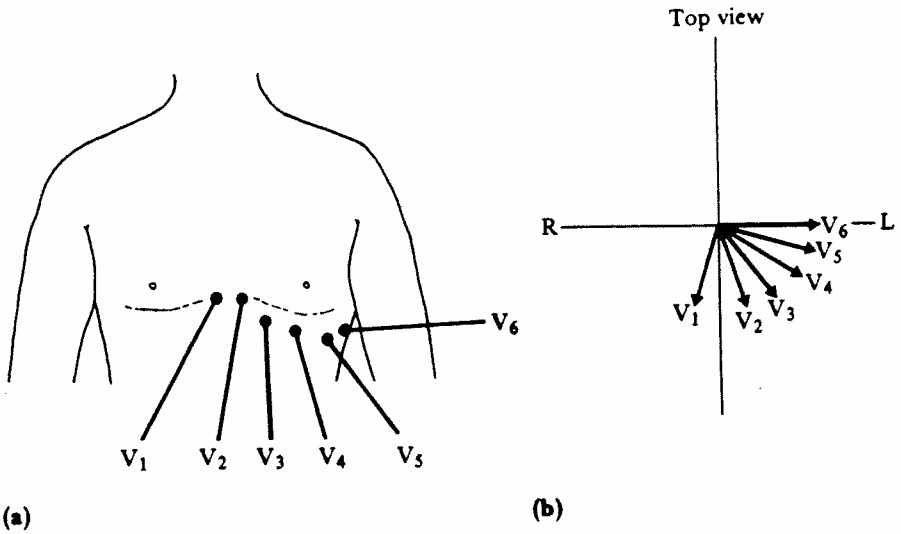


**Figure 6.6** (a) Positions of precordial leads on the chest wall. (b) Directions of precordial lead vectors in the transverse plane.

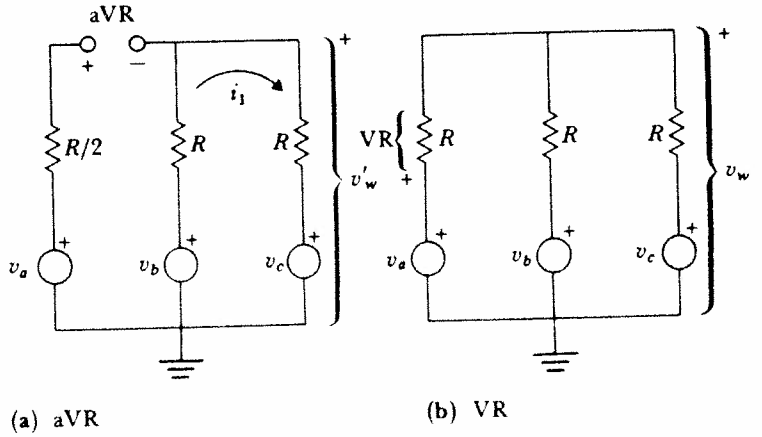


**Figure E6.1** Equivalent circuits for determining aVR and VR.

## 6.6 AMPLIFIERS FOR OTHER BIOPOTENTIAL SIGNALS

Up to this point we have stressed biopotential amplifiers for the ECG. Amplifiers for use with other biopotentials are basically the same. However, other signals do put different constraints on some aspects of the amplifier. The frequency content of different biopotentials covers different portions of the spectrum. Some biopotentials have higher amplitudes than others. Both these facts place gain and frequency-response constraints on the amplifiers used. Figure 6.20 shows the ranges of amplitudes and frequencies covered by several of the common biopotential signals. Depending on the signal,

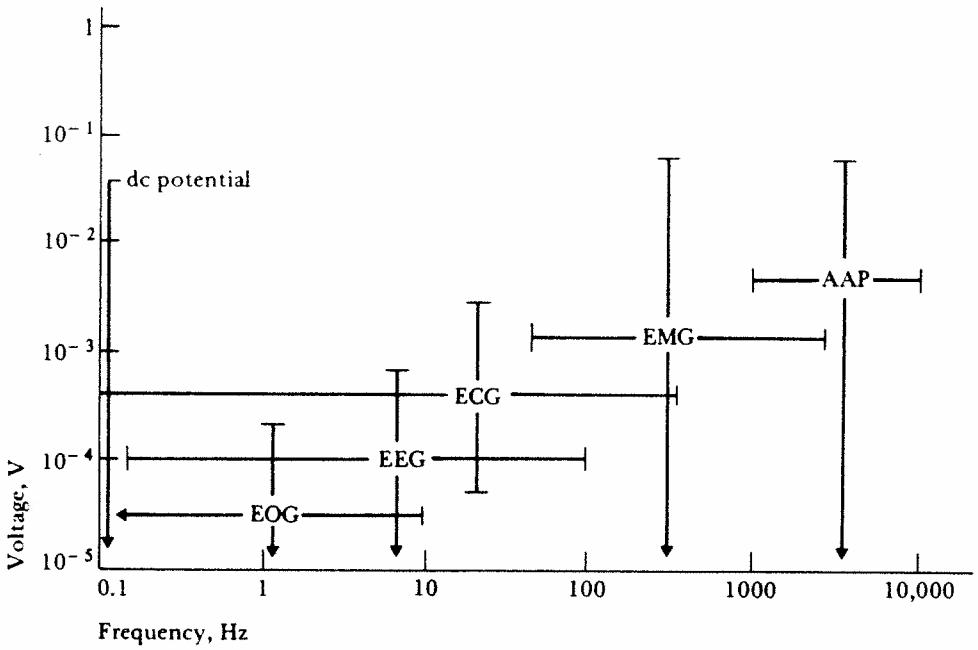


**Figure 6.20** Voltage and frequency ranges of some common biopotential signals; dc potentials include intracellular voltages as well as voltages measured from several points on the body. EOG is the electrooculogram, EEG is the electroencephalogram, ECG is the electrocardiogram, EMG is the electromyogram, and AAP is the axon action potential. (From J.M.R. Delgado, "Electrodes for Extracellular Recording and Stimulation," in *Physical Techniques in Biological Research*, edited by W.L. Nastuk, New York: Academic Press, 1964.

frequencies range from dc to about 10 kHz. Amplitudes can range from tens of microvolts to approximately 100 mV. The amplifier for a particular biopotential must be designed to handle that potential and to provide an appropriate signal at its output.

The electrodes used to obtain the biopotential place certain constraints on the amplifier input stage. To achieve the most effective signal transfer, the amplifier must be matched to the electrodes. Also, the amplifier input circuit must not promote the generation of artifact by the electrode, as could occur with excessive bias current. Let us look at a few requirements placed on different types of biopotential amplifiers by the measurement being made.

## EMG AMPLIFIER

Figure 6.20 shows that electromyographic signals range in frequency from 25 Hz to several kilohertz. Signal amplitudes range from 100 $\mu$V to 90 mV, depending on the type of signal and electrodes used. Thus EMG amplifiers must have a wider frequency response than ECG amplifiers, but they do not have to cover so low a frequency range as the ECGs. This is desirable because motion artifact contains mostly low frequencies that can be filtered more effectively in EMG amplifiers than in ECG amplifiers without affecting the signal.